DESIGN FOR A LOW-COST K-BAND COMMUNICATION SATELLITE CONSTELLATION

by

PEYTON DANIEL STRICKLAND

SEMIH OLCMEN, COMMITTEE CHAIR
JOHN BAKER
DOUGLAS BAYLEY

A THESIS

Submitted in partial fulfillment of the requirements
for the degree of Master of Science
in the Department of Aerospace
Engineering and Mechanics
in the Graduate School of
The University of Alabama

TUSCALOOSA, ALABAMA

2020

ABSTRACT

The feasibility of using a low-cost K-band communication satellite constellation in low-Earth orbit to provide continuous global coverage to ground terminal restricted aerospace vehicles was investigated. A phased array K-band transceiver pointing nadir, steerable ±45° in azimuth and elevation, and laser communication units for satellite-to-satellite cross link capability, were assumed for the payload. The figure of merit was the average percent coverage of the entire surface of the globe and the space surrounding the globe, up to 1000 km, with a goal of achieving 100% coverage, continuously.

The results indicate that continuous global coverage is not feasible with a heritage phased array K-band transceiver with a range of 2000 km and 72 satellites; however, a hypothetical phased array K-band transceiver with a range of 2975 km was able to provide continuous global communication. The low-cost goal was not realized. The estimated cost of the constellation with the hypothetical transceiver is $4.861 B due to the large command and data handling and power requirements associated with the K-band transceiver. With the enormous costs associated with this project, despite using commercially available products, further analysis of the proposed satellite constellation is not recommended.

DEDICATION

This thesis is dedicated to my family and friends. A special feeling of gratitude to my fiancé, Faith Alison Nolen, who has stood by my side every step of the way on the tumultuous road here these last five years and to my parents, Stephen, Robin, and Torrey Strickland, for the many sacrifices and words of encouragement offered along the way. I love you all.

LIST OF ABBREVIATIONS AND SYMBOLS

English Letters

A_s	sunlit surface area, m^2
A_{sa}	solar array area, m^2
A_r	ram area, m^2
B	blow-down ratio
B_m	magnetic field strength, T
c	speed of light, m/s
C	battery capacity, W-hr
c_d	drag coefficient
cm	center of mass, m
cp_a	center of aerodynamic pressure, m
cp_s	center of solar radiation pressure, m
D	degradation per year
DOD	depth of discharge, W/m^2
D_m	spacecraft's dipole moment, $A\text{-}m^2$
g_0	gravity at sea level, m/s^2
h	stored wheel momentum, N-m-s
I_d	inherent degradation
I_{sp}	specific impulse, s

I_y	moment of inertia about the y-axis, kg-m^2
I_z	moment of inertia about the z-axis, kg-m^2
L	satellite lifetime, years
L_d	lifetime degradation
L_t	thruster moment arm, m
$Life_{sat}$	satellite lifespan, years
M	Earth's magnetic constant, T-m^3
M_{acs_f}	attitude control system fuel, kg
M_f	dry mass, kg
M_{feed}	feed system mass, kg
M_p	propellant mass, kg
M_{press}	pressurant mass, kg
M_{tank}	propellant tank mass, kg
M_{thrust}	thruster mass, kg
N_b	number of batteries
N_s	number of satellites
n	transmission efficiency
P_{BOL}	beginning of life power, W/m^2
P_d	daylight power needed, W
P_e	eclipse power needed, W
P_{EOL}	end of life power, W/m^2
P_o	solar cell power output, W/m^2
P_{sa}	solar array power, W

q reflectance factor

R distance to Earth's center, m

S learning curve slope

S_{rate} wheel saturation rate, day(s)/sat

T thrust, N

T_a atmospheric drag torque, N-m

T_d length of daylight per orbit, s

T_e length of eclipse per orbit, hr or s

T_g gravity-gradient torque, N-m

T_m magnetic torque, N-m

T_s solar radiation pressure torque, N-m

$T1$ theoretical first unit cost, $

Tot_{cost} constellation cost, $

t_b burn time, s

V velocity, m/s

V_{p_loaded} loaded volume of fuel, L

V_{p_usable} usable loaded volume of fuel, L

V_{p_ullage} ullage volume, L

V_{total} total tank volume, L

X_e eclipse path efficiency

X_d daylight path efficiency

z altitude, m

Greek Letters

ΔV	change in velocity of spacecraft, m/s
Σ_{Pulses}	number of thruster firings
θ	sun incidence angle, ° (degrees)
θ_{vz}	angle between vertical and z-axis, ° (degrees)
λ	Magnetic latitude factor
μ	gravitational constant, m^3/s^2
ρ_{air}	density of air, kg/m^3
ρ_{fuel}	density of fuel, kg/m^3
ρ_{press}	density of pressurant, kg/m^3
φ	solar constant, W/m^2

Acronyms

ACS	Attitude Control System
ADCS	Attitude Determination and Control System
AER	Azimuth, Elevation, and Range
AFTS	Autonomous Flight Termination System
CERs	Cost Estimating Relationships
CONUS	Continental Estimating Relationships
ΔV	Delta-V
DoD	Department of Defense
DOD	Depth-of-Discharge
EOL	End-of-Life
GPS	Global Positioning System

GUI	Graphical User Interface
He	Helium
LEO	Low-Earth Orbit
NASA	National Aeronautics and Space Administration
PMD	Propellant Management Devices
RDT&E	Research, Development, Test, and Evaluation
RF	Radio Frequency
SMAD	Space Mission Analysis and Design
SRP	Solar Radiation Pressure
SSCM	Small Satellite Cost Model
STARS	Space-Based Telemetry and Range Safety
STK	Systems Tool Kit
TDRS	Tracking and Data Relay Satellite
TT&C	Telemetry Tracking and Command

ACKNOWLEDGEMENTS

I would like to express my gratitude for the support of my advisor, Dr. Semih Olcmen, and the other members of this thesis committee, Dr. John Baker and Dr. Doug Bayley, for their patience and support throughout the process of developing this thesis and during my time as an undergraduate and graduate student at The University of Alabama. I would not be where I am today without the unconditional support provided by these three individuals.

Furthermore, I would like to thank The MITRE Corporation for their support of my education through two internships and multiple learning opportunities. I am proud to say that I worked for such an incredible company. I would also like to thank Mr. Patrick Damiani, Mr. Jesse Griggs, and Mr. Rohan Thatavarthi for their support and guidance. Their counsel helped shape this project, especially the coverage analysis. I would also like to thank Lisa Valencia for taking time to talk to me about AFTS.

Lastly, I would like to thank the following people. First, thank you to Ms. Shannon Hubbard and Alabama Reach for supporting my educational endeavors and my emotional wellbeing. Thank you to my grandparents for your love and support and for showing me what it looks like to be an engineer. Thank you to Patrick, Scott, Lawrence, and Ember for always encouraging me to do better. You too Jerry! Thank you to the Nolen/Hayes/Hux family for all your love and support over these past five years. The efforts required during my educational career would not have been possible without your love and support.

CONTENTS

LIST OF TABLES

LIST OF FIGURES

INTRODUCTION

From Earth's surface to space, the United States is grappling with the challenges associated with securing its assets. Integrated communication, navigation, and surveillance are among the challenges faced by our nation as our space-based assets increase. Historically, a single multi-billion-dollar satellite has been acquired to carry-out a given mission; however, users are becoming increasingly aware of the benefits associated with the use of satellite constellations. Unlike a single satellite, constellations can provide continuous global or near global coverage. Furthermore, constellations provide resiliency as the mission can continue if a single satellite fails.

The concept of constellations is not novel. Russia first used a constellation with its Molniya satellites beginning in 1964. These satellites use highly eccentric orbits, which keep the Northern Hemisphere in view up to 16 hours a day (Johnson & Rodvold, 1993). From Molniya spy satellites, commercial companies amassed their own constellations—most notably, Iridium. The Iridium constellation provides L band voice and data connections over the entire globe, continuously (Iovanov et al., 2003). More recently, mega constellations for global internet coverage (Starlink and OneWeb) have been proposed and are currently being built. Thus, satellite constellations have been applied to several ventures. Still, the United States Government, primarily the National Aeronautics and Space Administration (NASA) and the Department of Defense (DoD), lacks a low-Earth orbit (LEO) constellation that can support its needs.

Currently, several aerospace vehicles are ground terminal restricted due to communication requirements. In order to expand communication capabilities, additional expensive ground stations must be built in diverse locations which can prove problematic. Furthermore, even when ground terminals are available for communication, re-entry objects such as a ballistic rocket face the same re-entry blackout issues that smaller capsule-type spacecraft encounter (Gillman et al., 2010). Two communication techniques can overcome blackout issues. First, increasing the frequency of the communications to one that is greater than the plasma frequency can solve the blackout problem (Lemmer, 2009). Second, ionization is not as prevalent on top of the spacecraft as the bottom due to the reentry angle making communication from above the spacecraft more desirable. While the plasma frequency greatly exceeds the frequency range of conventional S, C, and X band communication signals, higher frequency communications such as K-band may provide additional capability.

In addition to the communication issues that arise from aerospace vehicles performing missions such as delivering payloads to orbit, extended range vehicle testing for hypersonic or intercontinental ballistic missiles requires fixed or mobile instrumentation platforms (“pearls”) to be strung along (“string of pearls”) a few hundred kilometers to an entire ocean basin before those test flights can occur, which require multi-range cooperation (Burke, 2017). In 2017, a single test cost $160 million, and the open-air flight tests cost an average of up to $100 million (Smith, 2019). According to Burke, “The primary instrumentation drivers of the large number of required fixed and mobile instrumentation sites are flight termination systems and telemetry.” Thus, the cost of flight tests could be greatly decreased by the removal of the “string of pearls”. A satellite constellation capable of relaying telemetry at a high frequency such as K-band in conjunction with the use of autonomous flight termination systems could provide this capability.

Again, the concept of a satellite constellation for telemetry relay in conjunction with an autonomous flight safety system is not novel. In 2000, NASA began the Space-Based Telemetry and Range Safety (STARS) program in parallel with their Autonomous Flight Termination System (AFTS) as part of the Space Launch Initiative aimed at increasing safety and reliability and reducing the cost of a launch (Whiteman et al, 2005). STARS was envisioned to have a human-in-the-loop to send the abort signal for manned missions with telemetry data being relayed to the human-in-the-loop via NASA's Tracking and Data Relay Satellite (TDRS) constellation while AFTS was originally designed with no human-in-the-loop for unmanned missions through the use of an on-board autonomous self-destruct sequence via Global Positioning System (GPS) signals in correlation with inertial navigation system sensors as shown in Figure 1.

Figure 1. AFTS Concept Diagram (Valencia, 2019). AFTS does not utilize human-in-the-loop or over-head satellites for telemetry relay.

In 2003, the STARS program successfully demonstrated its ability to maintain a communication link with TDRS with the desired link margins for a supersonic aircraft (Whiteman et al., 2005); however, questions remain as to whether TDRS will meet future hypersonic and space transit vehicle data relay requirements as it has never been tested beyond supersonic aircraft (Spravka & Jorris, 2015). Furthermore, TDRS only provides "near constant" communication links (NASA, 2017). TDRS also experiences increased latency compared to LEO satellites due the larger distances required to transmit data from a geosynchronous orbit. In

2006, the STARS program was ended in favor of the AFTS due to AFTS exceeding expectations for space launch vehicles. AFTS was first tested in 2005 and used operationally by SpaceX in 2017. SpaceX also used AFTS in its first manned mission in May 2020. As a result of the success of AFTS, the United States Air Force implemented a strategy to transition to AFTS at the Eastern and Western Ranges by 2025 (Foust, 2020).

Since no satellite constellation in existence today has the ability to expand the communication capabilities of ground terminal restricted aerospace vehicles to meet the vehicle data requirements of up to K-band frequencies with continuous global communication, up to 1000 km in altitude, it is proposed a custom Iridium-like LEO satellite constellation capable of continuous communication links at K-band frequencies and laser communication cross-links between satellites be created. Other cross links such as radio frequency (RF) could work; however, laser communication has been chosen for this specific mission due to its data rate capabilities, communications range, and security. While the primary function of this constellation is to expand the communication capabilities of ground terminal restricted aerospace vehicles, the K-band frequency coupled with the use of AFTS on each test vehicle could also create a testing system wherein the need for "string of pearls" can be eliminated. The constellation would provide the ability to relay telemetry while AFTS would provide the flight termination as desired. With an expected satellite design life of 13 years, assuming the continuation of one test per year for conventional ballistic vehicles, modestly assuming one test per year for hypersonic vehicles as production efforts increase, and modestly assuming 50% of the $100 million cost per test is from the "string of pearls", the $1.3 billion that could be saved by the use of this constellation instead of the "string of pearls" could be allocated towards the cost of the constellation (Missile Defense Agency, 2019). Lastly, since the use of this satellite

constellation is applicable to NASA and several branches of the DoD, cost sharing could eliminate the burden of finding a single source to pay for the entire cost.

Due to time constraints and the author/public's lack of familiarity with hypersonic data rate and link budget requirements, the "string of pearls" concept has been left as a follow-on area of interest. Thus, this thesis will focus on the aerospace concepts and techniques required to create a constellation of satellites capable of achieving continuous global communication at K-band frequencies.

Reference Mission

In order to design a satellite and subsequent constellation capable of meeting the continuous global communication, up to 1000 km altitude, at K-band mission requirement, the communications payload and orbit must be chosen. To provide a low-cost, rapid solution, the initial analysis will attempt to use a heritage, commercially available K-band transceiver with applicable experience in this domain. If a heritage, commercially available transceiver will not meet the continuous global coverage requirements, a minimum transceiver range requirement will be derived to determine the capabilities needed for a hypothetical phased array K-band transceiver to meet the coverage requirements. With the help of The MITRE Corporation, the heritage, commercially available communication payload selected for each satellite consists of a phased array K-band transceiver with a range constraint of 2000 km pointing nadir, steerable $\pm 45°$ in azimuth and elevation, and laser communication units for satellite-to-satellite cross link capability. As the requirements for this constellation are very similar to the Iridium constellation (continuous global communication), the Iridium constellation orbit is used initially for the constellation orbit and modified as needed to fit this specific mission. The original Iridium constellation which provided continuous global coverage consisted of 66 satellites and six spares

divided among six orbital planes for a total of 72 satellites in orbit at an altitude of 780 km with an inclination of 86.4° (Iovanov et al., 2003). For the K-band communication constellation, 72 satellites divided among six orbital planes at an inclination of 85° will also be utilized. The orbital altitude of the K-band constellation will be optimized to provide maximum coverage capabilities at a minimum altitude based on the K-band transceiver capabilities. Since intercontinental aerospace vehicles have an apogee slightly less than 1000 km, no orbital altitudes below 1000 km will be considered so the objects of interest are always below the satellite (National Academy of Sciences, 2012). Lastly, the design life of each satellite is 13 years to allow the owner to maximize their use.

Satellite Design Model

The MATLAB computing language was chosen. Systems Tool Kit (STK) and SolidWorks are also integrated into the design process where applicable. The satellite design model consists of seven intermediary steps to size the subcomponents of the satellite. The eighth step uses The Aerospace Corporation's proprietary Small Satellite Cost Model (SSCM) to provide an accurate cost estimate of a single satellite and the constellation. A conceptual sketch of the design process is provided in Figure 2. The flow path of the design is marked by sequential steps, as follows:

Step 1 – coverage model to ensure constellation of satellites in orbit provides continuous global communication

Step 2 – satellite power requirements

Step 3 – power system model to produce battery and solar panel

Step 4 – satellite dry mass estimate

Step 5 – propulsion system model to produce thruster(s), propellant tank, and fuel requirements

Step 6 – satellite dimensions

Step 7 – attitude determination and control system (ADCS) model to produce reaction wheel and momentum dumping requirements

Step 8 – SSCM

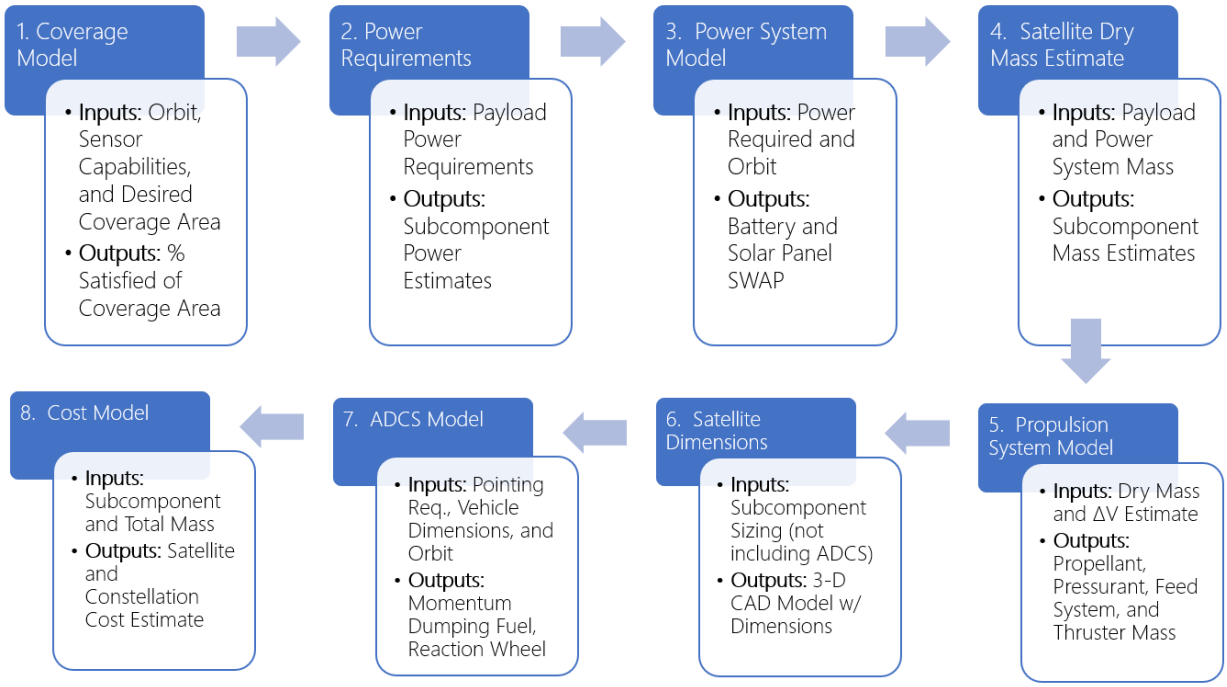

Figure 2. Graphical Representation of Satellite Design Process. Blue boxes indicate steps in the design process, and white boxes represent the inputs and outputs of each step

DESIGN CHOICES AND DESIGN ASSUMPTIONS

Design Choices

1. Reference mission
    a. 1000 km orbital altitude minimum

    Rationale: This altitude is slightly above the average apogee of an intercontinental aerospace vehicle; thus, only one K-band transceiver pointing nadir is needed as no intercontinental aerospace vehicle is likely to go above the satellite's orbital altitude. If for some reason one does, one of the satellites can use its reaction wheel to follow the object of interest.

    b. 72 satellites; six planes; 85° inclination

    Rationale: This is the Iridium constellation, a constellation that provides continuous global communication at the L-band, with slight modifications to adjust for a higher altitude. This constellation balances the revisit time of satellites over ground terminals, and the ability for cross communications between satellites with line-of-sight using laser systems.

    c. Area of interest equal to surface of globe and space surrounding the globe up to an altitude of 1000 km

    Rationale: The surface of the globe ensures that a satellite can communicate with any ground stations of interest. The space surrounding the globe between the surface of the globe and 1000 km altitude ensures that a satellite in the

constellation can communicate to any aerospace vehicle, up to the expected apogee of an intercontinental aerospace vehicle.

2. Reference heritage communications payload
    a. Phased array with a range constraint of 2000 km, steerable $\pm 45°$ in azimuth and elevation, and laser communication (6000 km range) for cross-links

       Rationale: Use realistic basis from The MITRE Corporation consultation.

    b. K-band Frequency

       Rationale: Use realistic basis from The MITRE Corporation consultation.

3. Power system model
    a. Deployable planar solar array

       Rationale: The variable and often high temperature of the solar cells is kept away from the payload.

    b. Triple junction gallium-arsenide (GaAs) solar cells

       Rationale: Triple junction GaAs solar cells have become the standard for most space applications due to their high efficiency and suitability for higher radiation environments.

    c. Lithium ion batteries

       Rationale: Rechargeable batteries will be required to allow the satellite to operate at full power during eclipses. Lithium-Ion was selected based on its significant volumetric and energy density advantages.

4. Propulsion system
    a. Monopropellant

Rationale: Use realistic basis from Space Mission Engineering: The New SMAD and a safety choice to reduce system complexity to improve mission reliability

b. Use of hydrazine for propellant

Rationale: Hydrazine is relatively stable under normal storage condition, high-performing (specific impulse), and commonly used.

c. Use of helium for pressurant

Rationale: Helium heats upon expansion alleviating the concern that pressurant lines may freeze. Helium is inert and has low volatility. Lastly, helium provides a reduced pressurant weight due to its molecular weight.

d. Four thrusters for momentum dumping

Rationale: Use realistic basis from Space Mission Engineering: The New SMAD.

e. One thruster for primary propulsion

Rationale: Use realistic basis from Space Mission Engineering: The New SMAD and to allow the satellite to get in its correct orbit upon release from the launch vehicle.

5. ADCS system

a. Star tracker determination sensor

Rationale: Laser communication systems often require pointing accuracy to $\mp 1°$ *which star trackers can provide.*

b. Fine sun sensor

Rationale: A sun sensor in conjunction with a star tracker providers redundancy of data and ability to help with determination during maneuvers such as detumbling

c. Four reaction wheels

Rationale: Three reaction wheels provide three-axis control and allow for a zero-momentum system (any momentum bias effects are regarded as disturbances). A fourth wheel provides redundancy in case one fails.

6. SSCM use

   Rationale: The Small Satellite Cost Model is a parametric cost model written and developed by The Aerospace Corporation. It is utilized by NASA, DOD, commercial contractors, universities, and foreign organizations for performing cost estimates of small spacecraft (up to 1000 kilograms).

Design Assumptions

1. Initial subcomponent power estimates are derived from historical data.

   Rationale: Use realistic basis from Space Mission Engineering: The New SMAD. The historical data provides % of total power used by each subcomponent. Furthermore, the historical data is broken down into four categories: No Propulsion, LEO Propulsion, High Earth, and Planetary. LEO propulsion was selected.

2. Initial subcomponent mass estimates are derived from historical data

   Rationale: Use realistic basis from Space Mission Engineering: The New SMAD. The historical data provides % of total mass used by each subcomponent. Furthermore, the historical data is broken down into four categories: No Propulsion, LEO Propulsion, High Earth, and Planetary. LEO propulsion was selected.

3. ΔV estimates are derived from historical data.

Rationale: Use realistic basis from Space Mission Engineering: The New SMAD. Figure 10-18 on page 253 provides the average boost, maintenance, and de-orbit ΔV requirement as a function of altitude.

COVERAGE MODEL

The goal of the coverage model is to ensure the proposed constellation of satellites in orbit provides continuous global communication, up to an altitude of 1000 km. As previously mentioned, a LEO satellite constellation of 72 satellites distributed among six orbital planes at an inclination of 85° was established. The altitude of the K-band constellation will be optimized to provide maximum coverage capabilities at a minimum altitude based on the K-band transceiver capabilities. The initial analysis will attempt to use a heritage, commercially available K-band transceiver with applicable experience in this domain. If a heritage, commercially available transceiver will not meet the continuous global coverage requirements, a minimum transceiver range requirement will be derived to determine the capabilities needed for a hypothetical K-band transceiver to meet the coverage requirements. The commercially available communications payload consists of a phased array K-band transceiver with a range constraint of 2000 km pointing nadir, steerable ±45° in azimuth and elevation, and laser communication units for satellite-to-satellite cross link capability.

Once the orbit and communications payload was established, a coverage model tool was created for the proposed satellite constellation using Analytical Graphics Incorporated's Systems Tool Kit (STK), a physics-based software package that allows engineers and scientists to perform complex analysis of ground, sea, air, and space platforms, through a MATLAB interface. STK allows the user to model the satellite constellation's parameters (orbit, number of satellites, etc.) and the K-band transceiver's parameters (field-of-view, range constraints, etc.).

Next, an area of interest or coverage zone can be designated. For the purpose of this thesis, the coverage zone was the entire surface of the globe and the space surrounding the globe, up to an altitude of 1000 km. STK then records the percentage of the coverage zone satisfied by time for the given scenario. The coverage model tool has been programmed into a MATLAB script which calls STK. If the initial orbit or communication payload does not allow continuous global communication, these properties can be easily changed. Then, the percentage of coverage zone satisfied by time can be recalculated by running the MATLAB code until 100% coverage of the area of interest is achieved. Finally, in order to ensure a satellite far away from a ground station is able to transmit information back to a given ground station, STK is utilized to ensure laser communication between satellites is always possible until a satellite with a view of a ground station is reached.

Methodology

First, a scenario was created in STK lasting for 24 hours to ensure redundancy of results through multiple completed orbits. The typical LEO orbital period is between 90 and 120 minutes. By running the scenario for 24 hours, several orbital periods are completed as the Earth is rotating which helps ensure the accuracy of the findings by computing the communications coverage over a variety of Earth orientations. Following this, the constellation of 72 satellites with an inclination of 85° was modeled. Since intercontinental aerospace vehicles have an apogee slightly less than 1000 km, no altitudes below 1000 km will be considered for the satellite constellation so the objects of interest are always below the satellite. Thus, the initial altitude of the satellites for the coverage model will be 1000 km. This altitude will be increased iteratively until continuous global coverage or the maximum coverage capable has been achieved for a given payload configuration.

A seed satellite, which is duplicated by STK to create the constellation, was modeled by inserting a default satellite at 1000 km with an 85° inclination. Next, the phased array K-band transceiver must be modeled onto the satellite. As there is not an easy way to perform a coverage analysis in STK with a phased array transceiver, the phased array transceiver was modeled as five simple conic sensors with each sensor having a half cone angle of 45° and range constraint of 2000 km. The first simple conic sensor pointed nadir while the other four simple conic sensors were angled at $\pm 45°$ in azimuth or elevation to reproduce the steering capability effects. Lastly, the Walker Tool in STK was utilized to create a Walker constellation, a group of satellites that are in circular orbits and have the same period and inclination, of 72 satellites which consisted of six planes with each plane having twelve replica satellites of the seed satellite. The Walker Tool requires two inputs: constellation type and interplane spacing. The "Star" configuration is selected for the Walker constellation type as it distributes the orbital planes over a span of 180° which helps to maximize global coverage. The interplane spacing, the advancement of the first satellite in a plane compared to the plane to the west as measured in orbital slots, was set at three through an iterative process which found this value maximizes available coverage under the current model assumptions.

Next, STK's Azimuth, Elevation, and Range (AER) Access Report feature can be utilized to ensure neighboring satellites are close enough together to allow communication between satellites via the on-board laser communication terminals (range of 6000 km). First, the satellite of interest is selected. Next, the satellites surrounding the satellite of interest are selected (four in total). Finally, the AER function is utilized which calculates the distance between the satellite of interest and its surrounding satellites as a function of time. If the maximum distance is less than 6000 km, the satellites are close enough for the laser communication terminals to work.

After the satellite constellation was modeled, “constellations”, a function within STK, can be utilized which allows a user to group a set of related objects, such as a group of sensors or satellites, into a single unit called a “constellation”. A satellite and sensor constellation are created. This makes it significantly easier to carry out a coverage analysis using a constellation as one can easily select all of the sensors as the assets of interest by simply choosing the sensor constellation for determining if the sensors have the ability to communicate to all of the globe’s surface.

Once the constellation object was created, a coverage grid is created in STK to assign the area of interest where coverage is important. The entire surface of the globe and the space surrounding the globe, up to 1000 km, were designated as the area of interest. As a result, the satisfied coverage area is calculated as a function of time by determining the area in which the transceiver can communicate, considering range and field of view constraints.

Finally, a “Satisfied by Time Report” was generated in STK and exported to an Excel file detailing the percentage of area covered as well as the total area covered in meters squared in single minute blocks during the 24-hour analysis period. This process is repeated for increasing constellation altitudes until continuous global coverage or the maximum coverage capable for a given payload configuration is achieved.

Coverage Model Output

With the coverage model finished, the program was run to determine the percentage of coverage over the area of interest as a function of time. A screenshot of the coverage grid in STK is shown below.

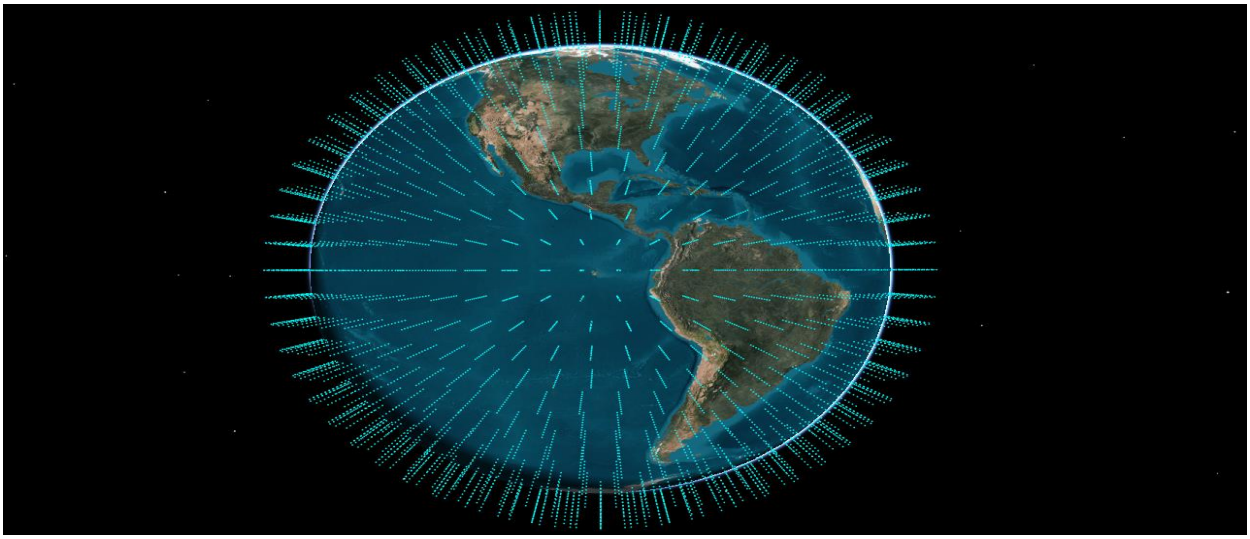

Figure 3. STK Coverage Grid

The coverage model process was iterated using this coverage grid and various constellation altitudes to find the maximum coverage capabilities for a given payload configuration. An example "Satisfied by Time Report" is shown below.

Time (UTCG)	% Satisfied	Area Satisfied (km^2)
45:00.0	86.27	5647121994
46:00.0	85.49	5596193253
47:00.0	85.37	5588659401
48:00.0	85.71	5610772362
49:00.0	85.51	5597843440
50:00.0	85.46	5594154202
51:00.0	85.53	5598748270
52:00.0	84.74	5547113080
53:00.0	86.51	5663265148
54:00.0	85.6	5603266692
55:00.0	84.58	5536382890
56:00.0	86.02	5631268057
57:00.0	85.11	5571107216
58:00.0	85.78	5615517197
59:00.0	85.46	5594626968
00:00.0	84.36	5522622664
Average	**85.44356003**	**5593232921**

Figure 4. Coverage Model Output

FIRST ORDER POWER ESTIMATES

Once the coverage model was completed, a first-order power estimate was generated. There are two approaches for determining a spacecraft's mass and power covered in *SME: The New SMAD* (Wertz & Larson, 2011). For the first approach, as described in section 14.7.1 "SCS Example" on page 432, one can begin with a target mass for the entire system and then determine the mass and power available for the spacecraft's subsystems. Conversely, as described in section 14.7.2 "FireSat II Example" on page 435, one can start with the payload and then determine the mass and power for the spacecraft. While the first method is great for flexible mission objectives, the FireSat II example is used in this analysis since the payloads of a K-band transceiver and laser communication units have already been defined by MITRE and the results of the coverage model.

Using Table 1

, the LEO with propulsion spacecraft section is used to generate a total power estimate.

Table 1

Average Power Percentage by Subsystem for 4 Types of Spacecraft (Wertz & Larson, 2011, Table 14-20)

Subsystem (% of Total Power)	No Propulsion	LEO Propulsion	High Earth	Planetary
Payload	43%	46%	35%	22%
Structure & Mechanisms	0%	1%	0%	1%
Thermal Control	5%	10%	14%	15%
Power (Incl. harness)	10%	9%	7%	10%
Telemetry, Tracking, & Command (TT&C)	11%	12%	16%	18%
On-board Processing	13%	12%	10%	11%
Attitude, Determination, & Control	18%	10%	16%	12%
Propulsion	0%	0%	2%	11%
Average Power (W)	299	794	691	749

According to the chart, 46% of the total power is used by the payload. With a total payload power consumption already known, the total power for the spacecraft is estimated by dividing the payload power by 0.46. This first-order estimate proves to be effective in that the final estimate for the power consumption of the satellite is relatively close to the final estimate that will be derived in the results section.

POWER SYSTEM MODEL

With a power requirement computed, a system to meet the power demand can be developed. The power system is comprised of two components: solar cells and batteries. There is a plethora of factors that influence the size and type of solar panels to be used. The first factor that affects the size needed is that the surface of the solar array may be eclipsed for extended durations of time depending on the satellite's altitude and inclination. Subsequently, the sunlight and eclipse periods for the satellite's defined orbit must be calculated to determine how much time the satellite's solar panels will have to collect sunlight. Furthermore, there are three types of solar cells that are generally used for satellite applications (gallium arsenide (GaAs), triple junction GaAs, and silicon). These three types of solar cells provide varying efficiency levels (higher efficiency, less area) and cost. As a result, the surface area of a solar panel needed to produce enough power to fulfill the satellite's power requirements require calculation for all three types to compare the surface area needed and the cost for each case to ensure that the optimal solution is being selected. Lastly, the batteries must be designed to store the energy derived from the solar panels. To accomplish this task, a MATLAB graphical user interface (GUI) linked to STK was created.

GUI Design

The first step in creating this model was to design a GUI that is easy to use. Designing the GUI first also defines the outputs for the MATLAB program that produces the results visualized on the GUI in an orderly manner which streamlines the coding process. Keeping in mind that conducting trade-studies is a key goal for this model, the GUI allows any user to

quickly view results for various power budgets, orbits, design life, and battery quantities. The GUI developed for this analysis is shown below.

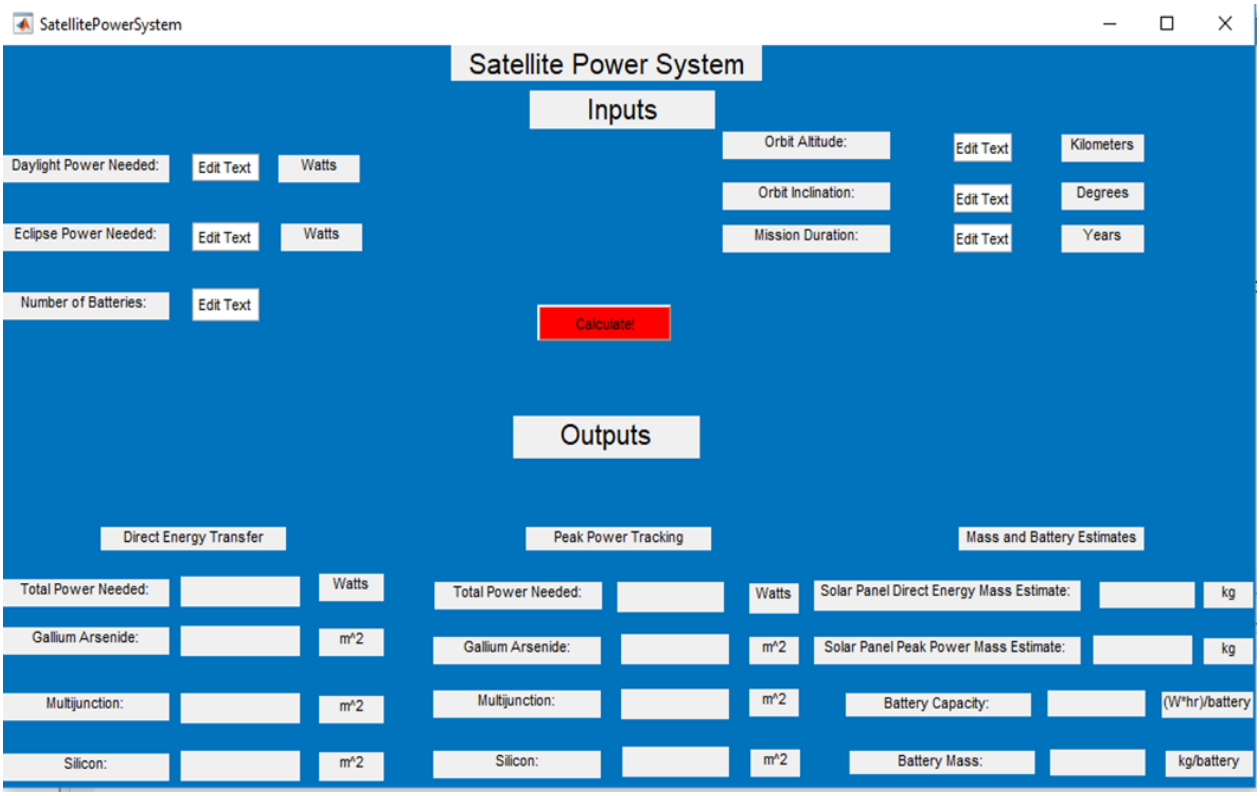

Figure 5. Satellite Power System GUI.

Solar Panel Sizing

For the program to calculate the solar panel area needed, the user first must input the following information: power needed during eclipse, power needed during daylight, orbit altitude, orbit inclination, and mission duration. This information is gathered from establishing a reference mission and by conducting a first order power estimate as shown in the previous section. Mission duration and the average power requirements are the two key design considerations in sizing the solar array because photovoltaic systems are sized at end-of-life (EOL) to ensure that adequate power can be supplied for the entire duration of the mission.

Once the following design parameters have been input, the power the solar array must provide during daylight to power the spacecraft along with recharging the batteries must be calculated as follows (Wertz & Larson, 2011):

$$P_{sa} = \frac{\frac{P_e T_e}{X_e} + \frac{P_d T_d}{X_d}}{T_d} \quad (1)$$

The terms X_e *and* X_d represent the efficiency of the paths from the solar arrays through the batteries to the individual loads and the path directly from the arrays to the loads, respectively. For direct energy transfer, the eclipse path efficiency and daylight path efficiency were approximated as 0.65 and 0.85, respectively; for peak-power tracking, eclipse path efficiency is estimated at 0.60 while daylight path efficiency is estimated at 0.80 by Wertz and Larson. The efficiencies of direct energy transfer are 5% greater than peak-power tracking because peak-power tracking requires a power converter between the arrays and the loads. STK was used to calculate the length of the eclipse and daylight periods per orbit, and the required power production from the solar array was calculated.

Generally, the third step in the solar array design process is the selection of the type of solar cell; however, since the model for this analysis is conducting a trade-study to determine the best solar cell balancing area and cost, all three solar cells were included. Table 2 details solar cell efficiencies for each type.

Table 2

Performance Comparison for Photovoltaic Solar Cells (Wertz & Larson, 2011, Table 21-13)

Cell Type	Silicon	Gallium Arsenide (GaAs)	Triple Junction GaAs
Theoretical Efficiency	29%	23.5%	40+%
Production Efficiency	22%	18.5%	30.0%

Best Laboratory Efficiency	24.7%	21.8%	33.8%

While silicon cells are mature in their development and can have lower cost in environments where radiation is not a concern, multijunction cells have become the standard for space applications despite their high cost. What makes them the best choice is their high efficiency resulting in less area required to produce the same amount of power comparative to silicon cells. Using the best laboratory efficiencies provided above, the power output for each solar cell is calculated by multiplying the efficiency by the solar constant 1,368 W/m^2.

Next, the beginning-of-life (BOL) power per unit area is determined using the following equation (Wertz & Larson, 2011):

$$P_{BOL} = P_o I_d \cos\theta \quad (2)$$

The solar cell power output calculation is provided in the previous step when the solar cell type is selected. Inherent degradation quantifies the loss in performance from design and assembly and is assumed to be 0.77 by Wertz and Larson. Lastly, the Sun incidence angle is the angle between the vector normal to the surface of the array and the Sun line. Although, the solar panel is configured to minimize this cosine loss, it is assumed by Wertz and Larson that theta is equal to 23.5 degrees in order to model an industry standard worst-case Sun angle assumption for LEO spacecraft to ensure power production requirements are always met.

The last step is the calculation of the EOL power per unit area which can then be used in conjunction with the solar array power calculated in the first step to calculate the area required (Wertz & Larson, 2011).

$$L_d = (1 - D)^L \quad (3)$$

$$P_{EOL} = P_{BOL} L_d \quad (4)$$

$$A_{sa} = \frac{P_{sa}}{P_{EOL}} \quad (5)$$

Several factors degrade a solar panel's performance. Lifetime degradation of the solar panel occurs due to thermal cycling, material degradation, and space debris impacts among others. First, the lifetime degradation can be calculated by Equation 3 for which the degradation per year for silicon, gallium arsenide, and multijunction are 3.75%, 2.75%, and 0.5%, respectively (Wertz & Larson, 2011). Next, the end-of-life power (Equation 4) was calculated using the beginning-of-life power and lifetime degradation. Finally, the solar array area can be calculated by dividing the solar array power by the end-of-life power, and the mass of the solar array is estimated by multiplying the solar array power by 0.04.

Battery Sizing

Energy storage plays a vital role in the electrical-power subsystem allowing the spacecraft to continue operating in eclipse periods and during peak-power demands. For the satellite under consideration with a thirteen-year design life, secondary (rechargeable) batteries were selected. Although nickel-cadmium and nickel-hydrogen are commonly used secondary batteries, lithium-ion was selected based on its significant volumetric and energy density advantages.

The spacecraft's orbital parameters, especially altitude, determine the number of charge/discharge cycles the battery must support. The depth-of-discharge (DOD) is limited to 30% for LEO spacecraft (Wertz & Larson, 2011). As a result, the cycle life is increased but the amount of energy available from the batteries during each cycle is decreased.

To determine the size of the batteries (battery capacity), only one equation is required (Wertz & Larson, 2011).

$$C = \frac{P_e T_e}{(DOD)(N_b)(n)} \quad (6)$$

The eclipse power and length of eclipse per orbit are defined in the solar panel sizing portion of the code. Next, the DOD is estimated at 0.30 based on the LEO orbit. Lastly, the number of batteries is generally set at two or more for redundancy, and the transmission efficiency is estimated at 90% by Wertz & Larson.

Power System Model Output

With all equations and variables defined, the power system model is complete. The solar array and battery information was outputted in the GUI that accomplishes the trade-study task. Figure 6 shows an example output.

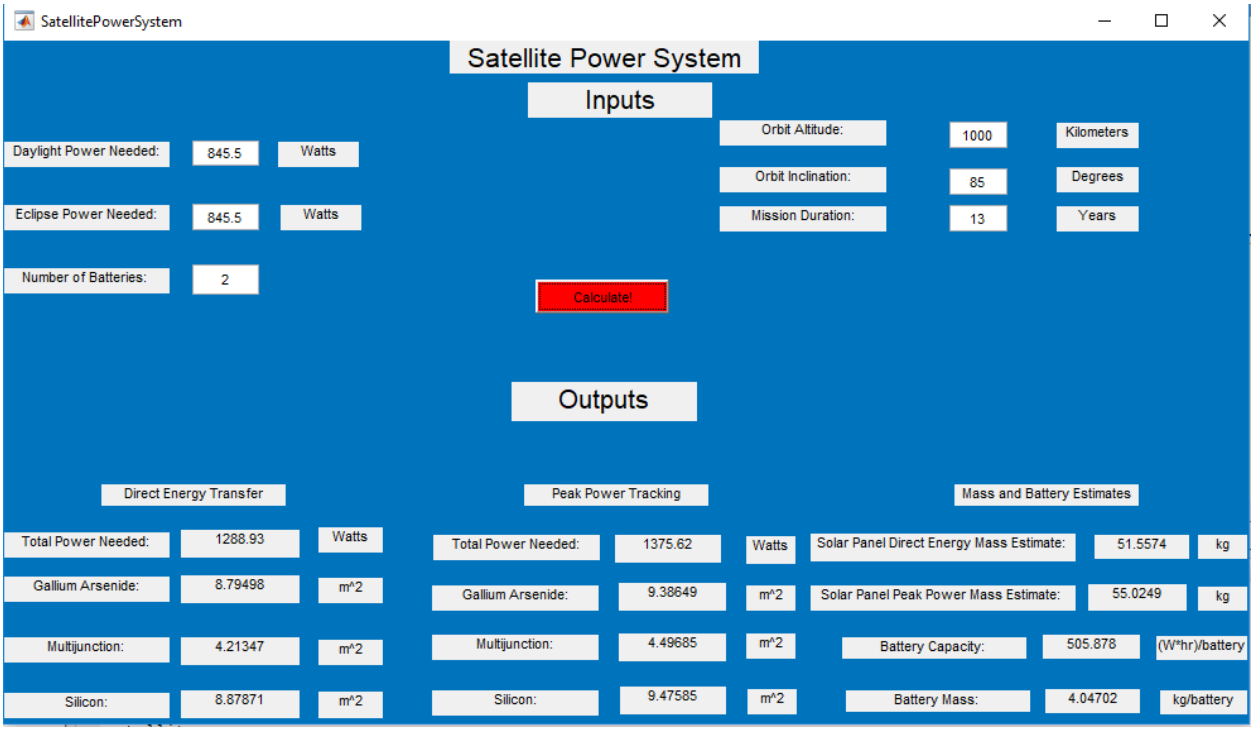

Figure 6. Satellite Power System Model Output.

FIRST ORDER MASS ESTIMATES

With first order estimates of the payload mass and power system mass, a first order dry mass estimate was derived so that the propulsion system could be designed. First, the payload total mass was calculated by adding the weight of the RF transceiver and the laser communication units. Once the payload mass was calculated, all other first order mass estimates, excluding the power mass estimate (which has already been calculated) were derived from the usage of Table 3.

Table 3

Average Dry Mass Percentage by Subsystem for 4 Types of Spacecraft (Wertz & Larson, 2011, Table 14-18)

Subsystem (% of Total Power)	**No Propulsion**	**LEO Propulsion**	**High Earth**	**Planetary**
Payload	41%	31%	32%	15%
Structure & Mechanisms	20%	27%	24%	25%
Thermal Control	2%	2%	4%	6%
Power (Incl. harness)	19%	21%	17%	21%
Telemetry, Tracking, & Command (TT&C)	2%	2%	4%	7%
On-board Processing	5%	5%	3%	4%
Attitude, Determination, & Control	8%	6%	6%	6%
Propulsion	0%	3%	7%	13%
Other (balance + launch)	3%	3%	3%	3%
Total	100%	100%	100%	100%
Propellant	0%	27%	72%	110%

The total dry mass was estimated by dividing the payload weight by the average percentage of dry mass for the payload subsystem. For this specific scenario, 64.5 kg would be divided by 0.31 (average payload percentage of dry mass for LEO spacecraft with propulsion) to calculate a total dry mass. Once this total dry mass has been estimated, the percentage for each

subsystem was multiplied by the total dry mass until all subsystems' masses were calculated. The total dry estimate listed in the results is slightly greater than the estimate provided using this method due to the power mass estimate from the satellite power system model being used instead of the 21% listed in Table 3. This increase in mass is to be expected as the power requirements for the satellite under design are greater than the average power requirements for a LEO satellite. Thus, no further research into this difference is needed as this is only a first order estimate.

PROPULSION SYSTEM MODEL

The goal of the propulsion system model is to calculate the mass of the propulsion system. First, the ΔV budget estimate must be obtained from the given orbital parameters. Using the spacecraft dry mass and ΔV budget estimates, the propellant mass can be solved for by rearranging the ideal rocket equation. Next, the mass of the tank, pressurant, and feed system can be calculated. Lastly, preliminary thrusters can be selected based on the mission requirements.

ΔV Estimate

Working with the rocket equation, the ΔV budget was used to create a propellant budget and estimate the propellant mass required for the space mission. Higher orbits require more propellant for orbit acquisition and de-orbit but less propellant for on-orbit maintenance. Once an orbital altitude is known, an accurate estimation method is needed. Figure 7 provides ΔV budget as a function of orbital altitude for LEO.

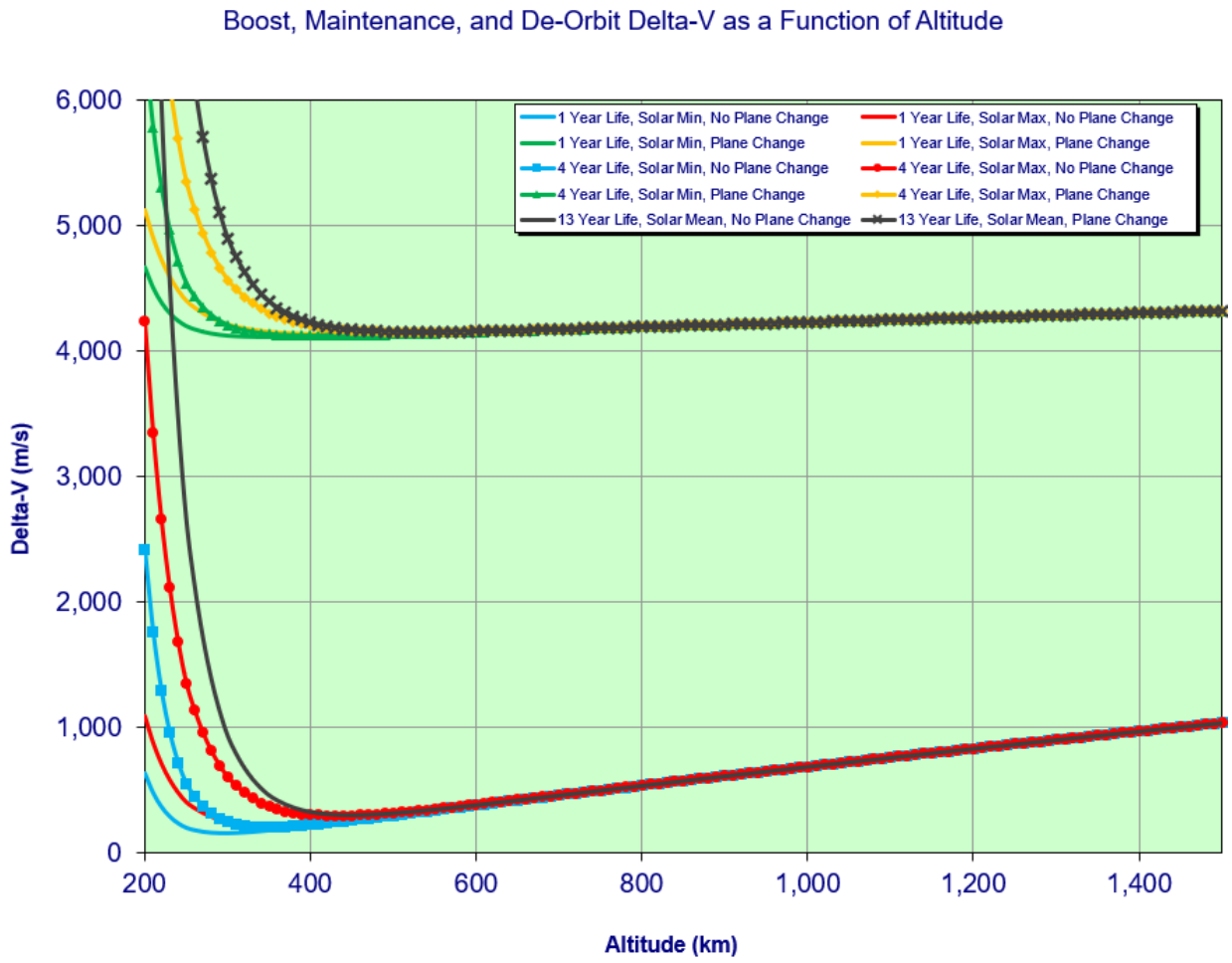

Figure 7. ΔV Budget Estimate (Wertz & Larson, 2011, Figure 10-16).

Propulsion System Mass Model

The spacecraft dry mass and ΔV budget estimates allow for the estimation of the propulsion system's mass. For preliminary design, the ideal rocket equation (Equation 7) was utilized to estimate the propellant mass.

$$M_p = M_f[e^{\Delta V/(I_{sp}g_0)} - 1] \quad (7)$$

The ΔV needed for boost, maintenance, and de-orbit is within the range for monopropellant thrusters. Subsequently, hydrazine was selected as the fuel resulting in a modest

I_{sp} estimate of 218 seconds. All remaining variables are known from previous calculations, and the propellant mass was computed.

Next, M_{p_usable} was defined as the propellant mass plus the fuel needed for attitude control. The fuel needed for attitude control is much smaller than the propellant mass needed to meet the ΔV, so for a first order estimate, it was assumed to be 9% of the total propellant mass. Not all the propellant loaded into a tank is usable however. As a result, a 3% margin is applied to the usable propellant to account for propellant trapped in the tank, feed lines, or valves (Brown, 2002). Furthermore, there is a measurement uncertainty of about 0.5% on propellant loaded. Thus, the total propellant loaded is as follows:

$$M_{p_{loaded}} = M_{p_{usable}}(1.0 + 0.03 + 0.005) \tag{8}$$

With the value of loaded propellant mass calculated, the propellant tank and feed system can be sized using the following equations (Wertz & Larson, 2011):

$$V_{p\_loaded} = {}^{M_{p\_loaded}}/_{\rho_{fuel}} \tag{9}$$

$$V_{p\_usable} = 0.97(V_{p\_loaded}) \tag{10}$$

$$V_{p\_ullage} = {}^{V_{p\_usable}}\Big/_{(B-1)} \tag{11}$$

$$V_{total} = 1.2(V_{p\_loaded} + V_{p\_ullage}) \tag{12}$$

$$M_{tank} = 2.7086e^{-8}{V_{total}}^3 - 6.1703e^{-5}{V_{total}}^2 + 6.629e^{-2}V_{total} + 1.3192 \tag{13}$$

$$M_{press} = \left(1.2V_{p\_ullage}\right)(.01\rho_{press}) \tag{14}$$

$$M_{feed} = 0.15\left(M_{p\_loaded} + M_{thrust} + M_{press}\right) - M_{tank} \tag{15}$$

First, the volume of fuel was calculated by dividing the loaded amount of propellant by the density of the fuel. The density of the fuel (Hydrazine) is 1.01 kg/L at 293 K (Wertz & Larson, 2011). As shown in Equation 8, not all the propellant mass will be utilized. It is estimated that

97% of the volume is full of usable propellant (Brown, 2002). Next, the ullage volume was calculated using the usable volume and the blow-down ratio. The blow-down ratio, defined as the final ullage volume over the initial ullage volume or the initial pressurant pressure over the final pressurant pressure, was assumed to be four, a typical value for modern blow-down propellant tanks. The final total volume was calculated adding the loaded volume and the ullage volume and adding a customary 20% margin. Finally, the tank mass is now sized using the final total volume and a curve fit of commercially available propellant management devices (PMD) propellant tanks as shown in Equation 13.

After computing the mass of the tank and the propellants, the mass of the pressurant and feed system require calculation. Currently, the initial operating pressure for the tank is unknown; however, an estimation was made from the operating pressure ranges of two candidate thrusters: MRE-1.0 and Monarc 445. The operating range for the MRE-1.0 is 0.055 to 3.9 MPa while the operating range for the Monarc 445 is 0.5 to 3.1 MPa (Northrop Grumman, n.d.; Moog, 2019). A 20% margin over the 3.9 MPa was carried so the initial pressure was estimated at 4.7 MPa and the initial temperature at 323 K. The pressurant selected was Helium (He). According to the NIST Chemistry WebBook, the density for He under those conditions is assumed to be 6.87 kg/m^3 (Linstrom & Mallard, n.d.). The equations (Equation 14 and 15) for the mass of the pressurant and the feed system can now be solved.

To complete the propulsion system model, the mass of the thrusters needed was estimated. For this specific scenario, four thrusters for unloading the excess momentum stored in the reaction wheels and one main thruster for primary propulsion were selected following the example of the FireSat II (Wertz & Larson, 2011). For the attitude control maneuvers, the candidate thruster selected was the flight-proven MRE-1.0. The MRE-1.0 has a mass of 0.5 kg,

average thrust of 3.4 N, and maximum thrust of 5.0 N. For the primary propulsion thruster, the potential candidate thruster is the Monarc-445 which has a mass of 1.6 kg and steady state thrust of 445 N. While the MRE-1.0 should meet thrust requirements for attitude control maneuvers, a final decision can be made after more information on thrust levels is gathered from the completion of the ADCS model as the ADCS model outputs the thrust required per momentum dump. If the MRE-1.0 is unable to meet the thrust requirement, a new engine can be selected, and the process can be iterated until the candidate thruster meets the thrust per momentum dump requirement.

FIRST ORDER ESTIMATE OF SATELLITE DIMENSIONS

A first order estimate of the satellite's dimensions and mass minus the attitude control system (ACS) are needed to size the ACS. With the first order mass estimates finalized and the size of several subsystems known a priori, the satellite's dimensions were calculated through a first order approximation process. Although, the ACS cannot be sized prior to the calculation, it constitutes a very small percentage of the overall size and mass of the satellite. As a result, the satellite was sized with a small portion of the volume reserved. To create an estimate of the satellite's dimensions, the author utilized an Excel spreadsheet to document the dimensions of each of the parts needed. With an Excel spreadsheet listing the dimensions of each part, SolidWorks, a solid modeling computer-aided design and computer-aided engineering computer program, can be utilized to create a 3D model to estimate the overall dimensions of the satellite body needed to store all the parts.

ATTITUDE DETERMINATION AND CONTROL SYSTEM (ADCS) MODEL

The final subsystem to be sized was the attitude determination and control system (ADCS). First, the determination sensors were selected based off the pointing requirements. Once the determination sensors were selected, the MATLAB model was initialized. The MATLAB model required vehicle, orbital, and Earth properties as inputs to generate the cyclical and secular angular momentum per orbit, a single reaction wheel mass, the fuel required for momentum desaturation of the reaction wheels over the satellite lifetime, and the thrust required for each momentum desaturation event.

Determination Sensors

The driving force behind the selection of the determination sensors was the pointing requirements of the payload. The RF transceiver described by MITRE has a 45-degree half-angle cone; however, the laser communication system does not have this ability afforded to it. Laser communication systems often require pointing accuracy to $\mp 1^{\circ}$. As a result, a star tracker was selected due to its ability to meet this accuracy requirement. Furthermore, a sun sensor was also selected in conjunction with the star tracker for redundancy of data and for its ability to help with determination during maneuvers such as detumbling.

Attitude Control System (ACS) Initiation Code

The purpose of the initiation file was to establish satellite properties and to call the functions that will determine the torques on the satellite and subsequently size the reaction wheels and thrusters accordingly. The vehicle properties utilized by the program included physical dimensions, center of gravity, mass, surface material code, and the lifespan of the

vehicle. Next, the orbital elements for the proposed satellite were input. The last information input was the properties of Earth. Finally, the ACS Sizing function was called by the ACS Initiation MATLAB script, and the torques and the ACS' size were estimated.

ACS Sizing Code

The ACS Sizing function requires inputs of the orbital elements, vehicle parameters, and planet parameters to compute the cyclical and secular angular momentum, the reaction wheel mass, the ACS fuel mass required, and the thrust required per momentum desaturation. Several steps are required to accomplish this task. First, the vehicle's 2^{nd} moment of inertia and the time for one orbit were calculated thereby enabling calculation and summation of the solar radiation, aerodynamic, magnetic, and gravity torques. This process was completed for the entire angular range of the orbit (0 to 360 degrees). Using the computed torques, the maximum torques around the orbit were integrated to find the total angular moment which was then used to find the cyclical and secular angular momentums. Lastly, the reaction wheel was sized using the cyclical angular momentum while the ACS propellant mass and thrust required for momentum desaturation were sized using the secular angular momentum. The calculated torques were displayed on a polar graph for visualization purposes as shown below in the "ACS Model Outputs" section.

Solar Radiation Pressure (SRP) Torque Calculation

Sunlight (i.e. photons) has momentum, and therefore exerts pressure when it strikes an object. The more absorptive the material, the more momentum absorbed resulting in a certain pressure force. If the sunlight is reflected, the pressure force felt is twice as much as the pressure force if all the sunlight is absorbed. While it is extremely difficult to estimate the true SRP because of the varying surfaces used on a satellite, a good first-order estimate can be made by

assuming uniform reflectance. With uniform reflectance assumed, the following equation is appropriate (Wertz & Larson, 2011):

$$T_s = \frac{\varphi}{c} A_s (1 + q)(cp_s - cm) \cos\theta \tag{16}$$

The solar constant was assumed to be 1,366 W/m^2. The surface material number was one of the inputs gathered at the beginning of the ACS Model. Using an Excel spread sheet, the MATLAB function gathered the reflectance factor (q) corresponding to the surface material number input by the user. Lastly, the angle of incidence of the sun was assumed to be zero degrees (worst-case). Listed below in Table 4 are the reflectance factors for possible spacecraft surface materials.

Table 4

Reflectance Factors for Commonly Used Spacecraft Materials (Fortescue et al., 2003)

Material Name	Material Number	Absorptance	Reflectance
Aluminized FEP	1	0.16	0.84
Aluminized Teflon	2	0.163	0.837
Aluminum Tape	3	0.21	0.79
Black Paint	4	0.95	0.05
Goldized Kapton	5	0.25	0.75
Optical Solar Reflector	6	0.07	0.93
Polished Beryllium	7	0.44	0.56
Quartz over Silver	8	0.077	0.923
Silver Coated FEP	9	0.08	0.92
Silver Paint	10	0.37	0.63
Silvered Teflon	11	0.08	0.92
Solar Cells, GaAs	12	0.88	0.12
Solar Cells, Silicon	13	0.75	0.25
Titanium (Polished)	14	0.6	0.4
White Paint (Silicate)	15	0.12	0.88
White Paint (Silicone)	16	0.26	0.74

Atmospheric Drag Torque Calculation

Just as photons have momentum and create pressure upon impacting a spacecraft, air particles also have momentum and create pressure when they impact a spacecraft. The density of air and pressure decrease exponentially with increasing altitude. As a result, only spacecraft in LEO encounter enough particles to justify an atmospheric drag torque calculation. The atmospheric drag was estimated by the following equation (Wertz & Larson, 2011):

$$T_a = \frac{1}{2}\rho_{air} C_d A_r V^2 (cp_a - cm) \quad (17)$$

Like SRP, when the center of atmospheric pressure, determined by the spacecraft area exposed to the atmosphere in the direction of the orbital velocity (i.e. ram direction), is not aligned with the center of mass, a torque occurs. The density of air is estimated using the 1976 U.S. Standard Atmosphere which provides the density from 0 to 1000 km. At 1000 km, according to the 1976 U.S. Standard Atmosphere, the density of air is 10^{-14} kg/m^3 (NASA, 1976). With 1000 km being the lowest altitude under consideration and with a lack of atmospheric models for altitudes greater than 1000 km, it is assumed that the density of air is 10^{-14} kg/m^3 for all altitudes under consideration. As density will continue to decrease as altitude increases, this density represents a worst-case scenario and likely an overestimation. The drag coefficient was estimated at a constant 2.2 (as is common practice for a LEO flying satellite (Wertz & Larson, 2011)). The ram area was calculated for the worst-case scenario by determining the largest area of all the sides. Lastly, the maximum distance from the aerodynamic center of pressure to the center of mass was calculated.

Magnetic Torque Calculation

The Earth's liquid core is a dynamo that induces a magnetic field. This magnetic field is strong enough to generate effects on the space surrounding Earth, so strong in fact that it

interacts with the satellite's weak magnetic residual moment. When the satellite's residual moment is not aligned to the local magnetic field from Earth, the satellite experiences a magnetic torque that attempts to align the two. The magnitude of this magnetic torque can be calculated using the equation presented in Equation 18 (Wertz & Larson, 2011).

$$T_m = D_m B_m = D_m \frac{M}{R^3} \lambda \tag{18}$$

This equation models the Earth's magnetic field as a dipole. The spacecraft's dipole moment is assumed to be 1 for a small, uncompensated spacecraft. Earth's magnetic constant is estimated at 7.18×10^{15} Tm^3. Lastly, lambda is a unitless function of the magnetic latitude that ranges from 1 at the magnetic equator to 2 at the magnetic poles.

Gravity-Gradient Torque Calculation

The final torque requiring computation was the gravity-gradient torque. Gravity-gradient torques arise when the spacecraft's center of gravity is not aligned with its center of mass with respect to the local vertical. The gravity-gradient torque increases as a function of the angle between the local vertical and the spacecraft's principal axes with the gravity-gradient torque always trying to align the minimum principal axis with the local vertical. Equation 19 provides a simplified equation for the gravity-gradient torque for a spacecraft with the minimum principal axis in its Z-direction (Wertz & Larson, 2011). Earth's gravitational constant of 3.986×10^{14} $\frac{\mathrm{m}^3}{\mathrm{s}}$ and a theta value equal to 45 degrees (i.e. worst-case scenario) are selected.

$$T_g = \frac{3\mu}{2R^3} |I_z - I_y| \sin 2\theta \tag{19}$$

Reaction Wheel Sizing

The reaction wheels were sized for cyclical momentum storage. To determine the mass of a reaction wheel, data was collected on several commercially available reaction wheels. With the data on the 28 commercially available reaction wheels gathered in a MATLAB script, a fourth-

order polynomial curve was fit to the data to compare the momentum storage capabilities of the reaction wheels and their weight in kilograms. From the polynomial curve, an approximate mass was estimated based off the momentum storage capabilities.

ACS Propulsion Sizing

The ACS propulsion sizing requires five inputs: the size of the spacecraft, the center of gravity, satellite lifetime, the saturation point of a reaction wheel (secular angular momentum), and the rate of saturation of a reaction wheel. These were used to compute the momentum dumping fuel mass required over the satellite lifetime and the thrust required for a single momentum dump. Although the proposed design includes four thrusters for momentum dumping and one main thruster, the ACS Propulsion Sizing code utilizes six thrusters (one on each side) and chooses the shortest moment arm which will require the largest thrust to design for the worst-case scenario. It is assumed that any thruster burn required for momentum dumping will fire for one second (Wertz & Larson, 1999).

With the worst-case moment arm calculated, the thrust required to dump the momentum is calculated (per pulse) using Equation 20 (Wertz & Larson, 1999).

$$T = \frac{h}{L_t t_b} \tag{20}$$

The propellant mass required for ACS over the satellite lifetime is then calculated with the following equations (Wertz & Larson, 1999).:

$$\sum_{Pulses} = \frac{3 \cdot Life_{sat} \cdot 365.25}{S_{rate}} \tag{21}$$

$$m_{acs\_f} = \frac{T \cdot \sum_{Pulses} \cdot t_b}{I_{sp} \cdot g_0} \tag{22}$$

$\sum_{Pulses}$ is the total number of thruster firings required throughout the lifetime of the spacecraft to ensure that the reaction wheels can control the attitude of the spacecraft. The numerator of Equation 21 has a factor of 3 because three reaction wheels will need to be desaturated each time a momentum dump is required. Lastly, since hydrazine was selected as the fuel of choice, the I_{sp} is 218 seconds (Wertz & Larson, 2011).

ACS Model Outputs

This completes the ACS model design process. In the Command Window of MATLAB, the following items are printed: cyclical angular momentum per orbit, secular angular momentum per orbit, reaction wheel mass, the fuel required for momentum dumping, and the thrust required per momentum dump. In addition, a polar graph showing the individual and total torques over the entire orbit is displayed. An example output screen is shown in Figure 8.

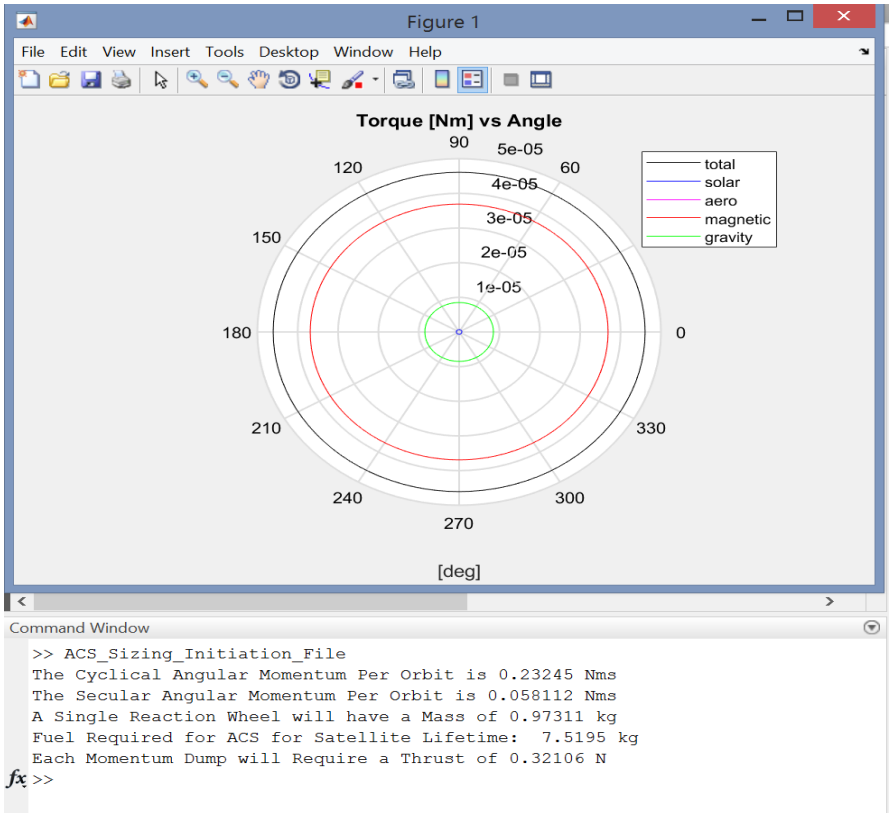

Figure 8. ACS Model Output.

COST MODEL

With the satellite designed, a parametric cost estimating model can be selected to price the constellation. A publicly available special purpose model was selected due to its free nature. While several publicly available special purpose cost estimating models are available, the Small Satellite Cost Model (SSCM) was selected because of its usefulness in pricing spacecraft weighing less than 1000 kg (The Aerospace Corporation, 2019). Developed by The Aerospace Corporation, it is assumed that these cost estimating relationships (CERs) include the cost of contractor program management, systems engineering, product assurance, and integration, assembly, and testing. The latest version (2019) of SSCM was acquired for use. Due to Export Administration Regulations, the details behind the latest CERs cannot be shared; however, Wertz & Larson (2011) provide a detailed review of the 1996 SSCM and its CERs. In addition to providing the equations, Wertz and Larson also provide an interactive Excel sheet for the 1996 version of the SSCM that is ready to use. Figure 9 presents a screenshot of the 1996 SSCM in Excel used to estimate the cost of the FireSat II spacecraft (Wertz & Larson, 2011).

User Inputs in Orange

Computation of Spacecraft computer source lines of code				
Kwords	bits/Kwords	Bytes/bit	SLOC/Byte (C code)	Source Lines of Code Converted from Kwords of Code:
781.35	16,384	0.125	0.02381	38,100

Learning Curve	
Number of Units Manufactured, N	2
Learning Curve Slope S =	0.95
B = 1 - (ln(1.0/S)/ln(2))	0.926
Learning Curve Multiplication Factor, L	1.90

Design Parameter	Mass (kg)	Average Power (W)	Percentage of Dry Mass
Payload	26.0	65.0	30.2%
S/C Subsystems	60.0	76.0	69.8%
ADCS	6.0	14.0	7.0%
C&DH	4.0	17.0	4.7%
Power	18.0	13.0	20.9%
Propulsion	4.0	0.0	4.7%
Structure	23.0	1.0	26.7%
Thermal	2.0	14.0	2.3%
TT&C (Comm)	3.0	17.0	3.5%
Margin	14.0	42.3	
Spacecraft Dry Mass	100.0	183.3	

Spacecraft Power Margin
30%

Small Spacecraft Cost Model											
Cost Component	CER Input Parameter	Value	Units	RDT&E plus 1st Unit Cost (FY10$K)	2nd Unit Cost (FY10$K)	Total Cost 2010 (FY10$K)	Total Cost 2012	Std Error ($K) 2010 (FY10$K)	Std Error ($K) 2012	Std Error Percentage**	SEE (FY$2010)
1.1 Spacecraft Bus											$3,696
1.1.1 Structure*	Mass	26.7	kg	$2,103	$1,893	$3,996	$4,119	$2,084	$2,149		$1,097
1.1.2 Thermal*		2.3	kg	$366	$329	$695	$716	$226	$233		$119
1.1.3 ADCS*	Mass	7.0	kg	$2,419	$2,178	$4,597	$4,739	$2,115	$2,180		$1,113
1.1.4 Electrical Power System*	Mass	20.9	kg	$3,553	$3,198	$6,752	$6,960	$1,729	$1,782		$910
1.1.5 Propulsion*	Spacecraft Bus Dry Mass	69.8	kg	$723	$651	$1,373	$1,416	$589	$607		$310
1.1.6a TT&C*	Mass	3.5	kg	$786	$707	$1,493	$1,539	$1,195	$1,232		$629
1.1.6b Command & Data Handling	Mass	4.7	kg	$1,255	$1,130	$2,385	$2,459	$1,623	$1,673		$854
1.1.7 Integration, Assembly, & Test (IA&T)	Spacecraft Bus Dry Mass	$11,206	FY10$K	$1,558	$1,402	$2,960	$3,051	$888	$915	30%	
1.1.9 Flight Software†	Source Lines of Code	38,100	N/A	$20,955	$0	$20,955	$21,601	$6,287	$6,480	30%	
Spacecraft Bus Total Cost				$33,719	$11,487	$45,206	$46,599	$7,522	$7,753		
1.2 Payload											
1.2.2 IR Sensor	Spacecraft Bus Total Cost	$11,206	FY10$K	$4,482	$4,034	$8,517	$8,779	$2,555	$2,634	30%	
2. Launch Segment	2 Minotaur Launches	$50,000	FY10$K	$25,000	$25,000	$50,000	$51,541	$5,000	$5,154	10%	
4. Program Level	Spacecraft Bus Total Cost	$11,206	FY10$K	$2,566	$2,310	$4,876	$5,026	$1,463	$1,508	30%	
5. Launch and Orbital Ops Support (LOOS)	Spacecraft Bus Total Cost	$11,206	FY10$K	$684	$615	$1,299	$1,339	$390	$402	30%	
6. Ground Support Equipment (GSE)	Spacecraft Bus Total Cost	$11,206	FY10$K	$740	$666	$1,405	$1,449	$422	$435	30%	
Total Space Segment Cost to Contractor				$41,507	$18,497	$60,004	$61,853				
10% Contractor Fee				$4,151	$1,850	$6,000	$6,185				
Total Space Segment Cost to Government				$45,658	$20,346	$66,004	$68,038				
Total Cost of Deployment						**$116,004**	**$119,580**	**9,517**	**$9,810**		

Figure 9. FireSat II SSCM Excel File.

To estimate the cost of the entire constellation (total lot cost), the following equation can be used (Wertz & Larson, 2011).

$$Tot_{cost} = T1 \cdot n_s{}^{\left(1+\frac{\ln S}{\ln 2}\right)} \tag{23}$$

The theoretical first unit cost is predicted by the SSCM Research, Development, Testing, and Evaluation (RDT&E) plus 1st Unit Cost estimate. The number of satellites is equal to the number of satellites in the constellation. Lastly, the learning curve slope factor, a term to account for the cost improvement observed as workers become more efficient and productive as more units of a nearly-identical product is produced, is estimated at 95% based on traditional learning theory estimates by Wertz and Larson.

While the SSCM predicts the development plus one protoflight unit cost, it does not predict the launch cost. As this research effort designs a constellation of 72 satellites, predicting the cost to launch all satellites is complicated. Table 11-23 “Historical Launch Vehicle Costs” in Wertz and Larson (2011) provides the mass capacity for several launch vehicles. The largest mass capacity of a vehicle still in use today is the Falcon Heavy. Using the mass capacity for the Falcon Heavy, a rough estimate can be made to determine how many satellites a single Falcon Heavy or similar launch vehicle could carry; however, caution should be used with this method. Volume constraints also become a concern when dealing with such a high quantity of satellites. After adding the SSCM estimate and the launch vehicle(s) cost, the design-to-orbit cost is complete.

VALIDATION EFFORTS

While the entire design cannot be validated due to its specific mission objectives, several of the developed models can be validated against the FireSat II spacecraft (Wertz & Larson, 2011). Overall, the satellite power system model, the propulsion system mass model, and the ADCS Model were validated.

Satellite Power System Model

An example test run was executed using the data provided by Table 21-12 "Solar Array Design Process" and Table 21-19 "Steps in the Energy Storage Subsystem Design" for the FireSat II spacecraft (Wertz & Larson, 2011). The results of the validation test are shown below.

Table 5

FireSat II Example Vs Satellite Power System Model

	FireSat II	Model	% Difference
Solar Array Area (m^2)	2.0	1.99	0.5
Solar Array Mass (kg)	9.6	9.42	1.88
Battery Capacity (W·hr)	119	116.34	2.24

The percent difference shown above is the result of the textbook using a rounded whole number for the silicon solar cell output and the Satellite Power System using a different length of daylight and eclipse per orbit than the values provided in Table 21-12. The Satellite Power System Model uses STK to determine the length of eclipse and the length of daylight per orbit. The length of daylight and length of eclipse for a satellite changes as the Earth's location relative

to the Sun changes. Since STK utilizes the date the program was run to determine the length of eclipse and the length of daylight, there is a slight variation in the values used. With a maximum difference of 2.24 %, the satellite power system has been verified to be accurate.

Propulsion System Mass Model

To verify the propulsion system mass model, data provided in section 18.8 of Wertz and Larson (2011) was utilized. Table 6 contains the results of the comparison between the FireSat II spacecraft and the model.

Table 6

FireSat II Example Vs Propulsion System Mass Model

	FireSat II	Model	% Difference
Tank (kg)	8.20	8.20	0.00
Feed System (kg)	3.60	3.60	0.00
Propellant (kg)	41.50	41.50	0.00
Pressurant (kg)	0.130	0.130	0.00

As expected, no difference exists between the two because the same equations were used, and no values were dynamically computed unlike the satellite power system where STK had to be used to solve for a daylight and eclipse period length that changes constantly based on the time period for the scenario of interest. Subsequently, the propulsion system mass model has been verified as being accurate when given the correct dry mass, ACS fuel estimate, and ΔV values.

ADCS Model

Verification of the ADCS model was made difficult due to the FireSat II spacecraft's lack of information directly related to using thrusters for momentum dumping. Upon researching

other potential verification methods, Wertz and Larson (1999) had information on the cyclical angular momentum per orbit and the fuel required for ACS for the original FireSat spacecraft. The numbers used for verification of the model are found in Table 11-13 “Simplified Equations for Preliminary Sizing of Thruster Systems” of Wertz and Larson.

Table 7

FireSat Example Vs ADCS Model

	FireSat	Model	% Difference
Cyclical Angular Momentum Per Orbit (Nms)	0.4	0.3815	4.625
ACS Fuel Required (kg)	2.43	2.38	2.06

The differences in Table 7 are due to two primary assumptions. First, the FireSat case study approximates the wheel momentum, h, through a simplified expression while the ADCS model integrates the worst-case disturbance torque over a full orbit. Second, in determining the ACS Fuel Required, the FireSat case study assumes the number of total pulses is known apriori whereas the ADCS model uses a simplified expression for the saturation rate to calculate the number of total pulses needed. While this verification has the highest percent difference, less than five percent difference is acceptable.

HERITAGE RESULTS

The results of designing a satellite constellation using the heritage, commercially available communication payload are presented. The results include the sizing of subcomponents through MATLAB code, a SolidWorks model of the satellite, and a cost model for the constellation. These results are duplicatable through the processes described in previous sections and through the use of the MATLAB code provided with this thesis in The University of Alabama Institutional Repository.

Heritage Transceiver Coverage Model Results

The results of the iterative trade-study are presented below.

Table 8

Heritage Transceiver (2000 km Range) Coverage Model Results

Altitude (km)	CONUS Average (%)	Global Average (%)
1000	89.83	85.44
1050	91.04	86.58
1100	91.50	86.93
1125	91.62	86.87
1150	91.39	86.69
1200	90.86	86.01
1250	89.94	84.93

As shown in Table 8, the heritage, commercially available phased array K-band transceiver is unable to provide continuous global coverage. The highest average percent coverage for the entire surface of the globe and the space surrounding the globe, up to 1000 km, was observed at a constellation altitude of 1100 km (86.93%). While one might think the coverage would continue to increase as altitude increases, the viewing area may increase directly below the satellite as altitude increases; however, the steerable coverage range on the sides of the satellite is decreased as altitude increases because of the fixed range of the phased array K-band transceiver. Thus, there is a trade-off in coverage between the area directly below the satellite and the area that can be seen when the transceiver beam is steered away from the nadir. The full design process is still carried out for the heritage transceiver to provide an idea of the cost of a system of this magnitude as a constellation capable of increasing the global coverage by approximately 13% will only further increase the price.

Heritage Transceiver Satellite Power Budget Results

Using the equations from Wertz and Larson (2011), a first order power estimate for the satellite was placed at 1,928 watts. This estimate is reasonably close to the following final power budget which was derived through the design iteration process.

Table 9

Heritage Transceiver Satellite Final Power Budget

Item	Watts (W)	Quantity	Total Power (W)
RF Transceiver	389	1	389
RF Transceiver Computer	178	1	178
ConLCT (Laser) (Motzigemba, 2016)	80	4	320
Reaction Wheels (Blue Canyon Tech., 2020)	6	4	24
Star Tracker VST-41M (Vectronic Aero., 2020)	2.5	1	2.5
Fine Sun Sensor (Bradford, 2017)	0.25	1	0.25
Main Thruster (Monarc-445)	58	1	58
Momentum Dumping Thrusters (MRE-1.0)	15	4	60
Thermal Control	192.8	1	192.8
On-Board Processing	231.36	1	231.36
Power (Regulation & Control, Distribution, etc.)	173.52	1	173.52
Structure and Mechanism	19.28	1	19.28
Total			**1,648.71**

As expected, these power estimates are also in family with the Iridium satellite's power requirements (~ 2 kW) (ESA Earth Observation Portal, 2020).

Heritage Transceiver Satellite Power System Results

Using the 1,648.71 watts estimate, the Satellite Power System model is used to calculate the solar array area, solar array mass, battery capacity, and battery mass. Figure 10 shows the results of the satellite power system model.

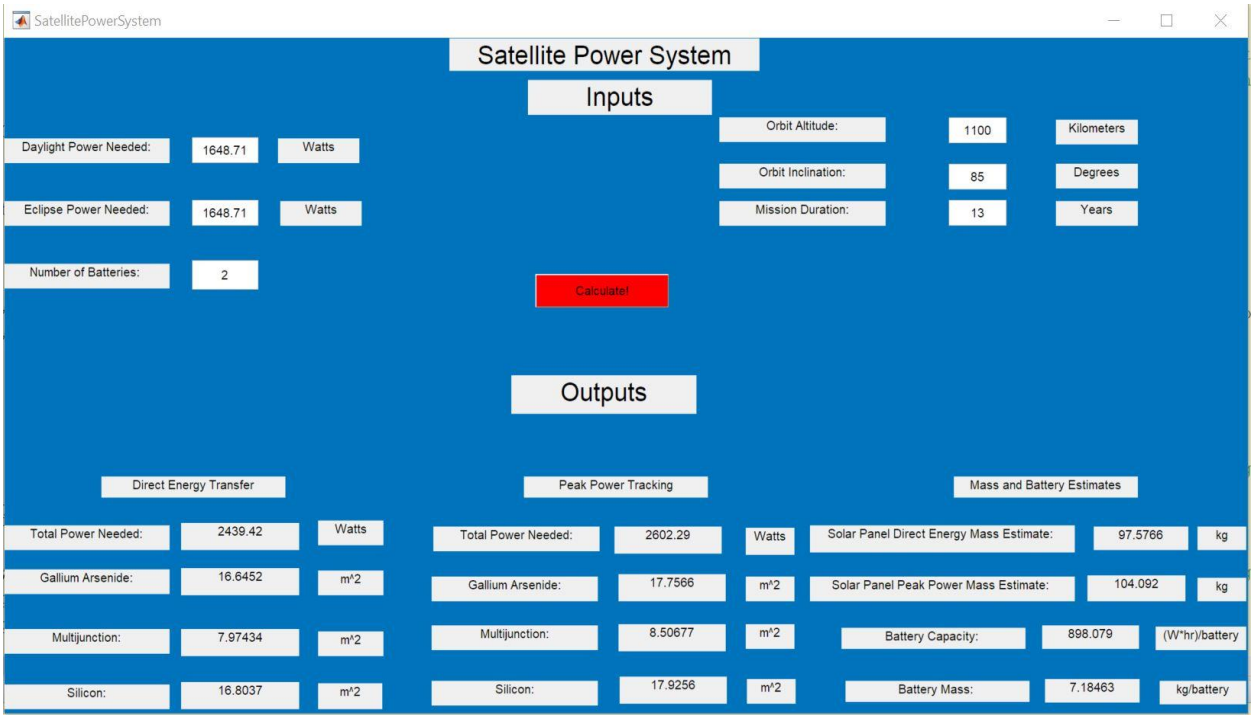

Figure 10. Heritage Transceiver Satellite Power System Results.

Based on these results, multi-junction cells using direct energy transfer were selected for the final design. An estimated 7.97 m^2 of solar array weighing 97.58 kg is required to meet the daylight and eclipse power requirements. Furthermore, to store the energy from the solar array, a battery with a capacity of 1,796.2 W·hr weighing 14.37 kg is needed.

Heritage Transceiver Satellite Mass Results

With the results from the coverage model and the satellite power system model, the spacecraft bus dry mass results using the equations from Wertz and Larson (2011) are shown below for the satellite designed with the heritage, commercially available transceiver.

Table 10

Heritage Transceiver Satellite Dry Mass Estimate Using SMAD Equations

Subsystem	Mass (kg)
Payload	64.5
Structure	56.25
Thermal	4.16
Power	111.95
TT&C	4.16
On-Board Processing	10.41
ADCS	12.49
Propulsion	6.24
Other	6.24
Total Dry Mass	276.40

Again, this dry mass estimation method proves extremely effective compared to the final dry mass estimate derived from a part list created after multiple iterations of the design process. Table 11 shows the final dry and wet mass estimates.

Table 11

Heritage Transceiver Satellite Dry and Wet Mass Results

Item	Mass (kg)	Quantity	Total Mass (kg)
RF Transceiver	2.27	1	2.27
RF Transceiver Computer	2.27	1	2.27
ConLCT (Laser)	15	4	60.0
Reaction Wheels (Blue Canyon Tech RWP500)	0.75	4	3.0
Star Tracker VST-41M	0.9	1	0.9
Fine Sun Sensor	0.375	1	0.375
Main Thruster (Monarc-445)	1.59	1	1.59
Momentum Dumping Thrusters (MRE-1.0)	1	4	4
Diaphragm Tank – PTD-222 (MT Aero., n.d.)	17.08	1	17.08
Propellant Feed System	10.41	1	10.41
Solar Panels	97.58	1	97.58
VES 180 Batteries (Saft, 2006)	1.11	10	11.10
Structure	56.21	1	56.21
Thermal Control	4.16	1	4.16
TT&C	4.16	1	4.16
On-Board Processing	10.41	1	10.41
Other (Balance+Launch)	6.25	1	6.25
Total Dry Mass			**291.77**
Propellant for ΔV Budget	130.69	1	130.69

Propellant for ACS	29.08	1	29.08
Pressurant Mass for Diaphragm Tank	0.42	1	0.42
Total Wet Mass			**160.19**
Total Mass			**451.96**

With a total mass of 451.96 kg, the satellite remains in the SSCM range (0-1000 kg).

Heritage Transceiver Satellite Dimensions

During the creation of the satellite's part list, the dimensions of each part is also recorded. Using this part list, a SolidWorks assembly was created to estimate the overall dimensions of the satellite, leaving a small portion of volume for parts whose size could not be easily estimated. The dimensions of the various parts and a picture of the SolidWorks assembly are shown below (Note: The solar panels are not shown).

Table 12

Heritage Transceiver Satellite Dimensions

Item	Dimensions (m or m^2)
RF Transceiver	Length: 0.127; Width: 0.089; Height: 0.165
RF Transceiver Computer	Length: 0.14; Width: 0.131; Height: 0.159
ConLCT (Laser)	Length: 0.25; Width: 0.20; Height: 0.10
Reaction Wheels (Blue Canyon Tech RWP500)	Length: 0.11; Width: 0.11; Height: 0.038
Star Tracker VST-41M	Length: 0.08; Width: 0.10; Height: 0.18
Fine Sun Sensor	Length: 0.108; Width: 0.108; Height: 0.0525
Main Thruster (Monarc-445)	Length: 0.41; Exit Diameter: 0.148
Momentum Dumping Thrusters (MRE-1.0)	Length: 0.188; Width: 0.114
Monopropellant Diaphragm Tank	Length: 1.027; Diameter: 0.608
Solar Panels	Area: 7.97
VES 180 Battery	Height: 0.25; Diameter: 0.053
Overall Dimensions (Structure):	Length: 1.25; Width: 0.724; Height: 0.724

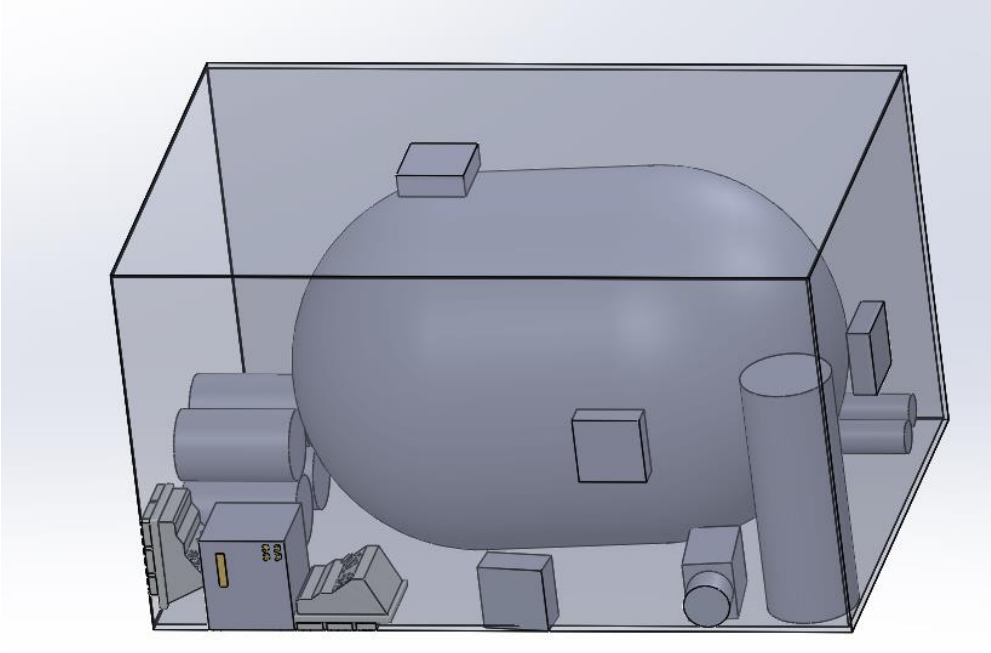

Figure 11. Heritage Transceiver Satellite SolidWorks Assembly.

Due to time constraints, some simplifications were made for a few of the part drawings. For example, the thrusters are simplified as cylinders. Lastly, as stated earlier, some of the volume is reserved for parts that could not be sized easily as shown in Figure 11.

Heritage Transceiver Satellite Cost Model

Finally, the SSCM was utilized to price the proposed satellite constellation. The estimated cost for the research, development, test, and evaluation (RDT&E) plus the first unit is $86.054 M in FY$2020 dollars while the estimated cost for the RDT&E and the building of the entire constellation is $4.515 B in FY$2020. This cost does not include the cost of launching the constellation into orbit.

An estimate for the cost of launching the constellation is also needed. The Falcon Heavy was selected as the launch vehicle. With the ability to take a payload mass of 63,800 kg to LEO, the Falcon Heavy could theoretically take all 72 satellites at an estimated cost of $130 M

(SpaceX, 2020; Wattles, 2019). While the mass can be taken, payload volume also becomes a concern; however, SpaceX does not publicly release mass-to-orbit capabilities for fairing configurations. Thus, the total launch cost is estimated at $200 M to provide a contingency fund of $70 M if a smaller rocket such as the Minotaur or Falcon 9 is necessary to finish launching any additional satellites after the launch of the Falcon Heavy. Finally, the design-to-orbit cost is calculated by adding the RDT&E, manufacturing, and launch costs and is estimated at $4.715 B.

HYPOTHETICAL TRANSCEIVER RESULTS

As previously shown, the heritage, commercially available transceiver is unable to provide continuous global coverage with 72 satellites at any altitude. Thus, a trade-study was executed to determine the minimum phased array K-band transceiver range capability required for the constellation of satellites to provide continuous coverage of the globe and the space surrounding the globe, up to 1000 km. The results of the trade study are presented in Table 13.

Table 13

Optimized Hypothetical Transceiver Coverage Model Results

Transceiver Range (km)	**"Winning" Altitude (km)**	**CONUS Average (%)**	**Global Average (%)**
2000	1100	91.50	86.93
2500	1350	99.78	99.62
2750	1400	99.978	99.984
2800	1400	99.990	99.993
2900	1400	99.9993	99.9992
2925	1400	99.9998	99.9996
2950	1400	100	99.9999
2975	1400	100	100

Thus, in order to provide continuous coverage of the area of interest with the proposed constellation, the phased array K-band transceiver range must be increased to 2975 km, and the constellation altitude must be 1400 km. A K-band transceiver with this range is not heritage. The lack of information about the size, weight, and power of a hypothetical transceiver with this range capability makes the modeling of such a satellite difficult. To provide an approximated answer, the size, weight, and power required for the hypothetical transceiver have been proportionally increased. For example, the power required for a range of 2000 km is 389 watts. To increase the range by 50% (2000 km to ~3000 km), the power requirement will also be increased by 50% from 389 watts to 583.5 watts. The RF transceiver computer will also have its size, weight, and power proportionally increased. While these results will not be exact, these results will provide an educated approximation. To create the desired results, the process completed in the "Heritage Results" section is duplicated.

Hypothetical Transceiver Satellite Power Budget Results

Using the equations from Wertz and Larson (2011), a first order power estimate for the satellite was placed at 2,545 watts. This estimate is reasonably close to the following final power budget which was derived through the design iteration process.

Table 14

Hypothetical Transceiver Satellite Final Power Budget

Item	Watts (W)	Quantity	Total Power (W)
RF Transceiver	583.5	1	583.5
RF Transceiver Computer	267	1	267
ConLCT (Laser)	80	4	320
Reaction Wheels (Blue Canyon Tech RWP500)	6	4	24
Star Tracker VST-41M	2.5	1	2.5
Fine Sun Sensor	0.25	1	0.25
Main Thruster (Monarc-445)	58	1	58
Momentum Dumping Thrusters (MRE-1.0)	15	4	60
Thermal Control	254.5	1	254.5
On-Board Processing	305.4	1	305.4
Power	229.05	1	229.05
Structure and Mechanism	25.45	1	25.45
Total			**2,129.65**

As expected, these power estimates are also in family with the Iridium satellite's power requirements (~ 2 kW) (ESA Earth Observation Portal, 2020).

.

Hypothetical Transceiver Satellite Power System Results

Using the 2,129.65 watts estimate, the Satellite Power System model is used to calculate the solar array area, solar array mass, battery capacity, and battery mass. Figure 12 shows the results of the satellite power system model.

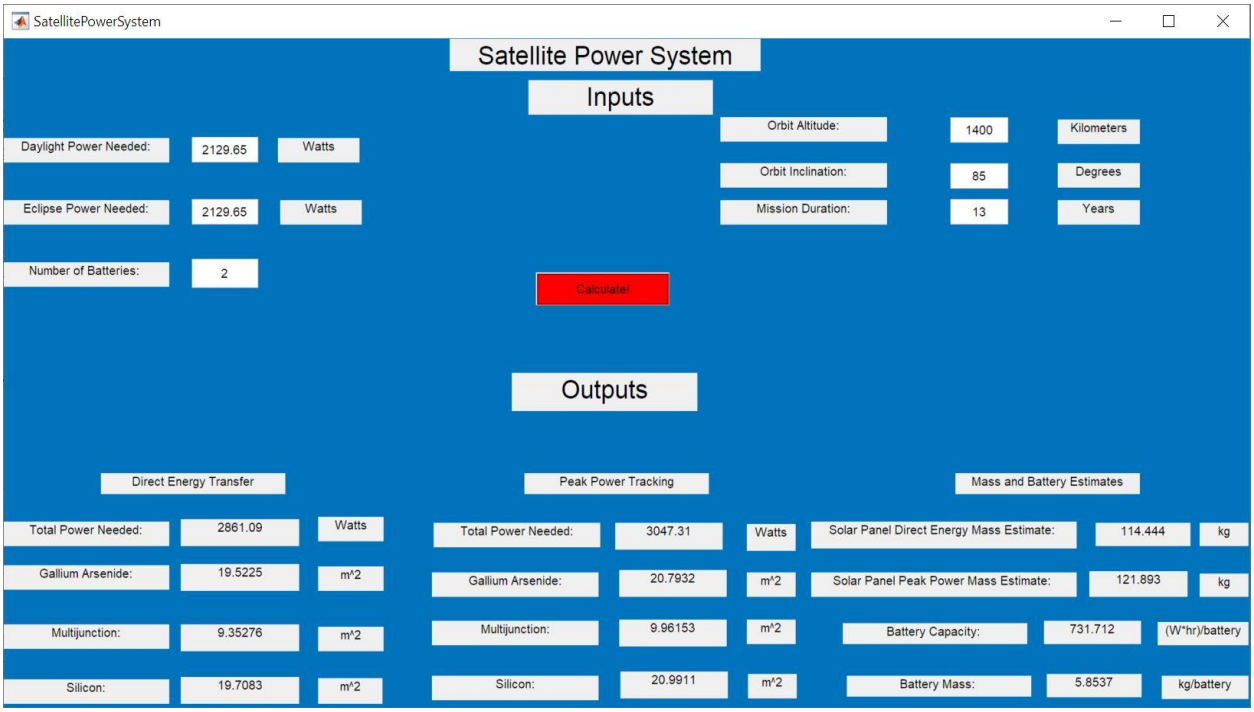

Figure 12. Hypothetical Transceiver Satellite Power System Results.

Based on these results, multi-junction cells using direct energy transfer were selected for the final design. An estimated 9.35 m^2 of solar array weighing 114.44 kg is required to meet the daylight and eclipse power requirements. Furthermore, to store the energy from the solar array, a battery with a capacity of 1,463.4 W·hr weighing 11.71 kg is needed.

Hypothetical Transceiver Satellite Mass Results

With the results from the coverage model and the satellite power system model, the spacecraft bus dry mass results using the equations from Wertz and Larson (2011) are shown below for the satellite designed with the hypothetical transceiver.

Table 15

Hypothetical Transceiver Satellite Dry Mass Estimate Using SMAD Equations

Subsystem	Mass (kg)
Payload	66.81
Structure	58.19
Thermal	4.31
Power	126.15
TT&C	4.31
On-Board Processing	10.78
ADCS	12.93
Propulsion	6.47
Other	6.47
Total Dry Mass	296.42

Again, this dry mass estimation method proves extremely effective compared to the final dry mass estimate derived from a part list created after multiple iterations of the design process. Table 16 shows the final dry and wet mass estimates.

Table 16

Hypothetical Transceiver Satellite Dry and Wet Mass Results

Item	Mass (kg)	Quantity	Total Mass (kg)
RF Transceiver	3.405	1	3.405
RF Transceiver Computer	3.405	1	3.405
ConLCT (Laser)	15	4	60.0
Reaction Wheels (Blue Canyon Tech RWP500)	0.75	4	3.0
Star Tracker VST-41M	0.9	1	0.9
Fine Sun Sensor	0.375	1	0.375
Main Thruster (Monarc-445)	1.59	1	1.59
Momentum Dumping Thrusters (MRE-1.0)	1	4	4
MILSTAR PMD Tank (Northrop Grumman, 2020)	20.2	1	20.2
Propellant Feed System	14.47	1	14.47
Solar Panels	114.44	1	114.44
VES 180 Batteries	1.11	9	9.99
Structure	58.19	1	58.19
Thermal Control	4.31	1	4.31
TT&C	4.31	1	4.31
On-Board Processing	10.78	1	10.78
Other (Balance+Launch)	6.47	1	6.47
Total Dry Mass			**319.84**
Propellant for ΔV Budget	190.97	1	190.97

Propellant for ACS	12.70	1	12.70
Pressurant Mass for Diaphragm Tank	0.53	1	0.53
Total Wet Mass			**204.20**
Total Mass			**524.04**

With a total mass of 524.04 kg, the satellite remains in the SSCM range (0-1000 kg).

Hypothetical Transceiver Satellite Dimensions

During the creation of the satellite's part list, the dimensions of each part is also recorded. As previously mentioned, the dimensions of the hypothetical transceiver and transceiver computer have been increased by 50% to compensate for the 50% increase in performance needed. The dimensions of the various parts are shown below.

Table 17

Hypothetical Transceiver Satellite Dimensions

Item	Dimensions (m or m^2)
RF Transceiver	Length: 0.191; Width: 0.1335; Height: 0.2475
RF Transceiver Computer	Length: 0.21; Width: 0.1965; Height: 0.2385
ConLCT (Laser)	Length: 0.25; Width: 0.20; Height: 0.10
Reaction Wheels (Blue Canyon Tech RWP500)	Length: 0.11; Width: 0.11; Height: 0.038
Star Tracker VST-41M	Length: 0.08; Width: 0.10; Height: 0.18
Fine Sun Sensor	Length: 0.108; Width: 0.108; Height: 0.0525
Main Thruster (Monarc-445)	Length: 0.41; Exit Diameter: 0.148
Momentum Dumping Thrusters (MRE-1.0)	Length: 0.188; Width: 0.114
MILSTAR PMD Tank	Diameter: 0.834
Solar Panels	Area: 9.35
VES 180 Battery	Height: 0.25; Diameter: 0.053
Overall Dimensions (Structure):	Length: 1.00; Width: 1.00; Height: 1.00

Hypothetical Transceiver Satellite Cost Model

Finally, the SSCM was utilized to price the proposed satellite constellation. The estimated cost for the research, development, test, and evaluation (RDT&E) plus the first unit was $88.827 M in FY$2020 dollars while the estimated cost for the RDT&E and the building of the entire constellation is $4.661 B in FY$2020. This cost does not include the cost of launching the constellation into orbit.

An estimate for the cost of launching the constellation is also needed. The Falcon Heavy was selected as the launch vehicle. Again, with the ability to take a payload mass of 63,800 kg to LEO, the Falcon Heavy could theoretically take all 72 satellites at an estimated cost of $130 M (SpaceX, 2020; Wattles, 2019). While the mass can be taken, payload volume also becomes a concern; however, SpaceX does not publicly release mass-to-orbit capabilities for fairing configurations. Thus, the total launch cost is estimated at $200M to provide a contingency fund of $70 M if a smaller rocket such as the Minotaur or Falcon 9 is necessary to finish launching any additional satellites after the launch of the Falcon Heavy. Finally, the design-to-orbit cost is calculated by adding the RDT&E, manufacturing, and launch costs and is estimated at $4.861 B.

SUMMARY AND CONCLUSIONS

In this thesis, the feasibility of using a low-cost K-band communication satellite constellation to provide continuous global coverage to ground terminal restricted aerospace vehicles was investigated. While a heritage phased array K-band transceiver was unable to provide the range necessary to allow for continuous global communication, a hypothetical phased array K-band transceiver with a range of 2975 km was able to provide continuous global communication.

The satellite design processes undertaken in this thesis provide insight into possible satellite design improvements. The primary objective has been generating useful results that can aid The MITRE Corporation and its sponsors in the systems engineering process at the preliminary design and verification level. The goals of the design process have been to optimize the cost of the satellite while at the same time meeting the desired performance requirements.

Upon review of the results, the satellite design does meet the requirements; however, the cost of the constellation ($4.861 B) is limiting. The initial goal for total constellation cost was between $500 M and $1 B. The large cost of the proposed constellation primarily stems from the command and data handling associated with K-band and the large power requirements associated with the transceiver. Because of its large cost, even with heritage components, further analysis is not recommended at this time. In the words of Retired Col. Scott Patton, “When an expensive satellite constellation is proposed, the question that must be answered is “What is its day job?” While the ability to use this constellation for test flights presents occasional use and cost-savings, the proposed constellation still does not warrant a budget equal in magnitude to the Global

Positioning Satellite constellation which is used daily by commercial and government consumers.

This optimized satellite design employs conventional forms of subsystem designs based on heritage satellite technology. It is likely that additional improvements in technology will develop between now and implementation of such a satellite. The use of composite materials along with improvements in monopropellants could bring about better performing and more cost-effective solutions. Regardless of technological advancements, the future of such a constellation will depend on the conceptualization and implementation of a useful daily task that the constellation can complete.

POTENTIAL IMPROVEMENTS

The following challenges in the thesis were noted:

1. The potential use of this constellation for the elimination of the “string of pearls” communication method was noted; however, a link budget could not be calculated as the data rate required for real-time hypersonic telemetry relay is not publicly known at this time. Upon dissemination of this information, a link budget could be completed to convert the transceiver range requirements to transceiver and ground equipment requirements. Some potentially useful information gathered on this subject has been included with this thesis in The University of Alabama Institutional Repository.
2. Another interesting solution for this problem is the use of laser communication for satellite to vehicle and satellite to ground communications. The primary issue with this concept is the large slewing requirements necessary for the laser to remain pointed at the target vehicle and vice-versa. The power requirements of the RF transceiver are almost a third of the total power budget. If the power budget could be reduced by a third, the solar panel area will decrease greatly which will also cause a significant decrease in the mass of the satellite. This mass savings will also decrease the mass of other systems allowing for a significant cost savings to occur.
3. The design method utilized provides a great point solution; however, the current design method does not quantify the design uncertainty due to the use of constants and approximations, thus hindering a truly optimized solution. Future studies that build upon the work in this thesis should include multidisciplinary design optimization to find the optimum

of the simultaneous problem instead of the optimum found by optimizing each discipline sequentially. For this effort, commercially available software tools such as OpenMDAO or non-gradient based evolutionary methods such as genetic algorithms, simulated annealing, or ant colony algorithms should be utilized to find the optimum of the simultaneous problem.

4. The SolidWorks drawing should be updated to include more accurate renderings of a few of the parts. Time constraints resulted in some approximation methods being utilized such as thrusters being approximated by a cylinder. More accurate renderings would allow for better visualization and center of mass approximations.

REFERENCES

Blue Canyon Technologies. (2020). *Reaction Wheels* [Fact Sheet]. https://storage.googleapis.com/blue-canyon-tech-news/1/2020/06/BCT_DataSheet_Components_ReactionWheels_06_2020.pdf

Bradford. (2017). *Fine Sun Sensor* [Fact Sheet]. https://www.bradford-space.com/assets/pdf/be_datasheet_fss_2017jan.pdf

Brown, C. D. *Elements of Spacecraft Design*. American Institute of Aeronautics and Astronautics. https://doi.org/10.2514/4.861796

Burke, A. (2017, January 25). Should We Continue to Rely on the String of Pearls [Conference Presentation]. 17th ITEA Engineering Workshop: System-of-Systems in a 3rd Offset Environment and the Directed Energy T&E Workshop, El Paso, TX, United States. http://itea.org/images/pdf/conferences/2017_SoS/Presentations/Burke.pdf

ESA Earth Observation Portal. (2020). *Iridium Next* [Fact Sheet]. https://directory.eoportal.org/web/eoportal/satellite-missions/i/iridium-next

Fortescue, P., Swinerd, G., and Stark, J. (Eds.). (2003). *Spacecraft Systems Engineering* (3rd ed.). John Wiley and Sons

Foust, J. (2020, September 15). *Polar Launches from Cape won't affect future of Vandenberg.* SpaceNews. https://spacenews.com/polar-launches-from-cape-wont-affect-future-of-vandenberg/

Gillman, E. D., Foster, J.E., and Blankson, I. M. (2010). *Review of Leading Approaches for Mitigating Hypersonic Vehicle Communications Blackout and a Method of Ceramic Particulate Injection Via Cathode Spot Arcs for Blackout Mitigation*. NASA/TM—2010-216220, Glenn Research Center.

Iovanov, M., Schulz, S. E., Dixon Jr., G.L., Puderbaugh, A. L., and Shepperd, R.W. (2003, September 23-25). Automation of Daily Tasks Necessary for the Management of a Large Satellite Constellation. *Proceedings of the AIAA Space 2003 Conference and Exposition*, Long Beach, California, AIAA 2003-6209. https://doi.org/10.2514/6.2003-6209

Johnson, N. L., and Rodvold, D.M. (1993). *Europe and Asia in Space: 1993-1994.* Kaman Sciences Corp., Colorado Springs, CO. https://apps.dtic.mil/dtic/tr/fulltext/u2/a338573.pdf

Lemmer, K. (2009). *Use of a Helicon Source for Development of a Re-entry Blackout Amelioration System* (Publication No. 63673) [Doctoral dissertation, University of Michigan]. UMich Campus Repository. https://deepblue.lib.umich.edu/handle/2027.42/63673

Linstrom, P.J., and Mallard, W.G. (n.d.). *NIST Chemistry WebBook, NIST Standard Reference Database Number 69*. National Institute of Standards and Technology, Gaithersburg, MD. https://doi.org/10.18434/T4D303

Missile Defense Agency. (2019, September). *Ballistic Missile Defense Intercept Flight Record* [Fact Sheet]. https://www.mda.mil/global/documents/pdf/testrecord.pdf

Moog. (2018). *Monopropellant Thrusters* [Fact Sheet]. https://www.moog.com/content/dam/moog/literature/Space_Defense/spaceliterature/propulsion/Moog-MonopropellantThrusters-Datasheet.pdf

Motzigemba, M. (2016, October 17). Commercial and Military Capabilities of Optical Satellite Communications Terminals. *Proceedings of the 2016 26th International Communications Satellite Systems Conference (ICSSC),* Cleveland, Ohio. http://proceedings.kaconf.org/papers/2016/clq/3_1.pdf

MT Aerospace (n.d.). *Spacecraft Propellant Tanks* [Fact Sheet]. https://www.mt-aerospace.de/downloadcenter.html?file=files/mta/tankkatalog/MT-Tankkatalog_01b_4-3_03.pdf

National Academy of Sciences. (2012). *Making Sense of Ballistic Missile Defense: An Assessment of Concepts and Systems for U.S. Boost-Phase Missile Defense in Comparison to Other Alternatives.* The National Academies Press.

National Aeronautics and Space Administration. (2017, September 7). *Tracking and Data Relay Satellite (TDRSS).* https://www.nasa.gov/directorates/heo/scan/services/networks/tdrs_main

National Aeronautics and Space Administration. (1976, October 1). *U.S. Standard Atmosphere, 1976.* NASA-TM-X-74335. https://ntrs.nasa.gov/citations/19770009539

Northrop Grumman. (n.d.). *MRE-1.0 Monopropellant Thruster* [Fact Sheet]. https://www.northropgrumman.com/wp-content/uploads/MRE-10_MonoProp_Thruster.pdf

Northrop Grumman. (2020). *PMD Tanks Data Sheets—Sorted by Volume* [Fact Sheet]. https://www.northropgrumman.com/space/pmd-tanks-data-sheets-sorted-by-volume/

Smith, R. J. (2019, June 19). Hypersonic Missiles are unstoppable. And They're Starting a New Global Arms Race. *The New York Times Magazine.* https://www.nytimes.com/2019/06/19/magazine/hypersonic-missiles.html

SpaceX. (2020). *Falcon Heavy* [Fact Sheet]. https://www.spacex.com/vehicles/falcon-heavy/

Saft. (2006). *Rechargeable Li-on Battery Systems* [Fact Sheet]. https://www.custompower.com/documents/VES.pdf

Spravka, J. J. and Jorris, T. R. (2015). *Current Hypersonic and Space Vehicle Flight Test and Instrumentation*. Air Force Test Center Edwards AFB., Edwards AFB, CA. https://apps.dtic.mil/dtic/tr/fulltext/u2/a619521.pdf

The Aerospace Corporation. (2010). *Small Satellite Cost Model.* https://aerospace.org/sscm

Valencia, L. M. (2019, September 16-17). Autonomous Flight Termination System (AFTS) [Conference Presentation]. 59th Meeting of the Civil GPS Service Interface Committee, Miami, FL, United States. https://www.gps.gov/cgsic/meetings/2019/valencia.pdf

Vectronic Aerospace. (2020). *Star Tracker VST-41M* [Fact Sheet]. https://www.vectronic-aerospace.com/wp-content/uploads/2020/03/VAS-VST41M-DS5.pdf

Wattles, J. (2018, June 21). *SpaceX's massive Falcon Heavy rocket lands $130 million military launch contract*. CNN Business. https://money.cnn.com/2018/06/21/technology/future/spacex-falcon-heavy-launch-contract-military/index.html

Wertz, J. R., and Larson, W. J. (1999). *Space Mission Analysis and Design*. Microcosm Press.

Wertz, J. R., and Larson, W. J. (2011). *Space Mission Engineering: The New SMAD*. Microcosm Press.

Whiteman, D. E., Valencia, L. M., and Simpson, J. C. (2005, October 25-27). Space-Based Range Safety and Future Space Range Applications. *Proceedings of the 1st International Association for the Advancement of Space Safety (IAASS) Conference*, Nice, France. https://ntrs.nasa.gov/search.jsp?R=20050238489